Characterization of fluorescent proteins, promoters, and selectable markers for applications in the Lyme disease spirochete *Borrelia burgdorferi*.

Constantin N. Takacs[1,2,3], Molly Scott[1,2,3] and Christine Jacobs-Wagner[1,2,3,4,*]

[1] Microbial Sciences Institute, Yale West Campus, West Haven, CT, 06516, USA.
[2] Department of Molecular, Cellular, and Developmental Biology, Yale University, New Haven, CT, 06511, USA.
[3] Howard Hughes Medical Institute, Yale West Campus, West Haven, CT, 06516, USA.
[4] Department of Microbial Pathogenesis, Yale School of Medicine, New Haven, CT, 06536, USA

* To whom correspondence should be addressed. Tel: +1 203 737-6778; Fax: +1 203 737-6715; Email: christine.jacobs-wagner@yale.edu.

ABSTRACT

Lyme disease is the most widely reported vector-borne disease in the United States. Its incidence is rapidly increasing and disease symptoms can be debilitating. The need to understand the biology of the disease agent, the spirochete *Borrelia burgdorferi*, is thus evermore pressing. Despite important advances in *B. burgdorferi* genetics, the array of molecular tools available for use in this organism remains limited, especially for cell biological studies. Here, we adapt a palette of bright and mostly monomeric fluorescent proteins for versatile use and multi-colour imaging in *B. burgdorferi*. We also characterize two novel antibiotic selection markers and establish the feasibility of their use in conjunction with extant markers. Lastly, we describe a set of constitutively active promoters of low and intermediate strengths that allow fine-tuning of gene expression levels. These molecular tools complement and expand current experimental capabilities in *B. burgdorferi*, which will facilitate future investigation of this important human pathogen.

INTRODUCTION

Lyme disease, a widespread infection transmitted by hard ticks of the *Ixodes* genus, is the most prevalent vector-borne disease in the United States. The condition is also common in Europe and Asia, and its incidence and geographic distribution have been steadily increasing in recent decades (1). Lyme disease is caused by spirochetal bacteria belonging to the *Borrelia burgdorferi* sensu lato group, with *B. burgdorferi* sensu stricto (from here-on referred to as *B. burgdorferi*) being the principal agent in North America, and *B. afzelii* and *B. garinii* being the primary agents in Eurasia. In humans, acute Lyme disease is often associated with a characteristic skin rash and flu-like symptoms. If left untreated, late stages of infection may result in carditis, neurological manifestations, and arthritis (2).

Spirochetes in general, and the *Borrelia* species in particular, display cellular features unusual for bacteria (3). Spirochete cells are typically very long and thin by bacterial standards. *B. burgdorferi* cells, for example, are 10 to 25 μm long and ~ 250 nm wide (4-6). Spirochetes are also highly motile, but, unlike in most bacteria, their flagella are not external organelles (7). Instead, their flagella are located in the periplasm (i.e., between the inner and outer membranes). In *B. burgdorferi*, the helicity of the flagella imparts the flat-wave morphology of the bacterium (8). *B. burgdorferi* also possesses what is likely the most segmented genome of all bacteria analysed to date. It is made up of a linear chromosome of about 900 kilobases (kb) and over 20 linear and circular genetic elements ranging from 5 to 60 kb in length (9,10). These smaller genetic elements are often referred to as plasmids, though many of them encode proteins that are essential for the life cycle of this organism (11). Recent work from our laboratory has shown that *Borreliae* species also have an uncommon pattern of cell wall synthesis in which discrete zones of cell elongation in one generation predetermine the division sites of daughter cells in the next generation (6).

While these unusual cellular features are integral to *B. burgdorferi* physiology and pathogenesis, little is known about how they arise or are maintained over generations. In fact, the cell biology of this pathogen remains largely unexplored. Technical hurdles have slowed progress in this area. Genetic manipulation of *B. burgdorferi* is feasible, but the available genetic tools are still limited, and the process remains cumbersome (12,13). Constitutive gene expression is mostly limited to the use of very strong promoters. Moreover, apart from a few exceptions (14-19), fluorescent protein reporters have primarily been used as gene expression reporters or as cellular stains for *in vivo* localization of the spirochete (13). Yet fluorescent proteins have many more uses, which have transformed the field of cell biology (20). For example, fluorescent proteins have opened the door to localization studies in live cells. They have also facilitated the detection of protein-protein interactions, the measurement of physical

properties of the cell, and the analysis of single events and of population heterogeneity. Much of this information is not accessible through the use of bulk biochemical measurements on cell populations. The averaging inherent to such techniques leads to loss of spatial resolution and obscures rare events and cell-to-cell or subcellular heterogeneity of behaviour (21). Indeed, the ability to perform extensive genetic manipulations and to use a wide panel of fluorescent proteins in an organism has been key to progress in understanding bacterial cell biology (22). Such approaches have been extensively used in model bacteria such as *Bacillus subtilis*, *Escherichia coli*, and *Caulobacter crescentus* since the first reported use of fluorescent protein fusions two decades ago (23-25). In order to facilitate the study of *B. burgdorferi*, we have generated new investigative tools by characterizing a panel of fluorescent proteins, promoters and antibiotic resistance markers for use in this medically important bacterium.

MATERIAL AND METHODS

Bacteria, growth conditions, and genetic transformations

Bacterial strains used in this study are listed in Table 1. *E. coli* strains were grown at 30 °C in liquid culture in Super Broth medium (35 g/L bacto-tryptone, 20 g/L yeast extract, 5 g/L NaCl, 6 mM NaOH) with shaking, or on LB agar plates. Plasmids were transformed by electroporation or heat shock. For selection of *E. coli* strains we used 200 µg/mL (solid medium) or 100 µg/mL (liquid medium) ampicillin, 20 µg/mL (solid medium) or 15 µg/mL (liquid medium) gentamicin, 50 µg/mL kanamycin (solid and liquid media), 50 µg/mL spectinomycin (solid medium), 50 µg/mL streptomycin (liquid medium), and 25 µg/mL (liquid medium) or 50 µg/mL (solid medium) rifampicin.

B. burgdorferi strains were grown in BSK-II medium supplemented with 6% (vol/vol) heat inactivated rabbit serum (Sigma Aldrich or Gibco) or in complete BSK-H medium (Sigma Aldrich), as previously described (26-28). Cultures were incubated at 34 °C under 5% CO_2 atmosphere in a humidified incubator. Antibiotics were used at the following concentrations (unless otherwise indicated): gentamicin at 40 µg/mL, streptomycin at 100 µg/mL, kanamycin at 200 µg/mL, blasticidin S at 10 µg/mL, and hygromycin B at 250 µg/mL. Ampicillin was purchased from Fisher Scientific, blasticidin S and hygromycin B from Invivogen, and all other antibiotics and biliverdin hydrochloride from Sigma Aldrich.

89 **_B. burgdorferi_ strain generation**

90 *B. burgdorferi* electrocompetent cells were prepared as previously described (29) and were
91 transformed with shuttle vector plasmid DNA (usually 30 μg) by electroporation. Electroporated cells
92 were then allowed to recover overnight in BSK-II medium at 34 °C. The next day, antibiotic selection
93 was initiated and 5-fold serial dilutions of the culture were plated in a 96-well plate (24 wells for each
94 dilution). After 10-14 days of incubation, the wells were inspected by microscopy using dark-field
95 illumination. When fewer than 20% of the wells of a given dilution were positive for growth, those wells
96 were considered to contain clonal populations and were further expanded and characterized. When
97 appropriate, fluorescence imaging was used to confirm fluorescent protein expression. Alternatively,
98 selected, non-clonal transformant populations were enumerated using C-Chip disposable
99 hemacytometers (INCYTO), using the manufacturer's instructions with the following change: counting
100 was done by continuously scanning the full height of the counting chamber for each counting surface to
101 account for the height of the counting chamber being larger than the size of the spirochetes. Enumerated
102 spirochetes were then diluted in BSK-II media and plated in 96-well plates at an average density of 0.2
103 cells/well. After 10-14 days, clonal growth was confirmed by dark-field microscopy imaging.
104
105 **Determination of minimal inhibitory concentrations (MIC) and antibiotic cross-resistance**
106 MICs were determined using strains B31 e2 or B31 MI, while cross-resistance testing was done
107 using B31 e2-derived strains that contained shuttle vectors carrying kanamycin, gentamicin,
108 streptomycin, blasticidin S, or hygromycin B resistance markers (see strains CJW_Bb069 through
109 CJW_Bb073 in Table 1). For both tests, antibiotics were two-fold serially diluted in complete medium.
110 For each concentration, 100 μL of antibiotic solution were dispensed into two to four wells of 96-well
111 plates. The cell density of *B. burgdorferi* cultures was determined by direct counting using dark-field
112 microscopy. The cultures were then diluted to 2×10^4 cells/mL in antibiotic-free medium, and 100 μL of
113 this diluted culture were added to the antibiotic-containing wells to yield an inoculum of 10^4 cells/mL.
114 The plates were incubated for at least 4 days at 34 °C under 5% CO_2 atmosphere in a humidified
115 incubator, after which each well was checked for spirochete growth and motility using dark-field
116 microscopy. A well was marked as positive if motile cells were detected. The plates were further
117 incubated for several days, during which bacterial growth-dependent acidification caused the phenol-red
118 pH indicator in the medium to change colour. This colour change was documented using colourimetric
119 trans-illumination imaging on a GE Amersham Imager 600. We verified that growth scoring of each
120 well by dark-field imaging matched the observed medium colour change.
121

DNA manipulations

Plasmids used in this study are listed in Table 2. Methods of plasmid construction and sequences of oligonucleotide primers are provided as Supplementary Data. Standard molecular biology techniques were used, as detailed in the Supplementary Data. Codon optimisation was performed using the web-based Java Codon Adaptation Tool hosted at www.jcat.de (30), using the codon usage table for *B. burgdorferi* as stored at www.kazusa.or.jp/codon (31). Codon-optimised DNA sequences were then chemically synthesized at Genewiz. DNA sequences of each codon-optimised gene are provided in the Supplementary Data. The names of these genes include a *Bb* superscript to indicate that the gene's nucleotide sequence is codon-optimised for translation in *B. burgdorferi* (e.g. $iRFP^{Bb}$). The name of the protein encoded by such a gene (e.g. iRFP), however, does not include the Bb superscript, as the protein's amino acid sequence does not differ from that expressed from other versions of the gene.

Microscopy

Visualization and counting of live spirochetes were done using a Nikon Eclipse E600 microscope equipped with dark-field illumination optics and a Nikon 40X 0.55 numerical aperture (NA) phase contrast air objective. Phase contrast and fluorescence imaging was done on a Nikon Eclipse Ti microscope equipped with a 100X Plan Apo 1.40 NA phase contrast oil objective, a Hamamatsu Orca-Flash4.0 V2 Digital CMOS camera, a Sola light engine (Lumencor), and controlled by the Metamorph software (Molecular Devices). Alternatively, light microscopy was performed on a Nikon Ti microscope equipped with a 100X Plan Apo 1.45 NA phase contrast oil objective, a Hamamatsu Orca-Flash4.0 V2 CMOS camera, a Spectra X light engine (Lumencor) and controlled by the Nikon Elements software. Excitation of iRFP was achieved using the 640/30 nm band of the SpectraX system, but higher excitation efficiency and thus brightness could in theory be obtained using a red-shifted excitation source between 660 and 680 nm. The following Chroma filter sets were used to acquire fluorescence images: CFP (excitation ET436/20x, dichroic T455lp, emission ET480/40m), GFP (excitation ET470/40x, dichroic T495lpxr, emission ET525/50m), YFP (excitation ET500/20x, dichroic T515lp, emission ET535/30m), mCherry/TexasRed (excitation ET560/40x, dichroic T585lpxr, emission ET630/75m), and Cy5.5 (excitation ET650/45x, dichroic T685lpxr, emission ET720/60m). For imaging, cultures were inoculated at densities between 10^3 and 10^5 cells/mL, and were grown for two to three days to reach densities between 10^6 and $3x10^7$ cells/mL. The cells were then immobilized on a 2% agarose pad (6,32) made with phosphate buffered saline covered with a No. 1.5 coverslip, after which the cells were immediately imaged live. Images were processed using the Metamorph software. Figures were generated using Adobe Illustrator software.

Image analysis

Cell outlines were generated using phase contrast images and the open-source image analysis software Oufti (33). Outlines were checked visually for each cell and were extended manually to the full length of the cells when appropriate. When not assigned to single cells or assigned to non-cellular debris, outlines were manually removed. The remaining outlines were automatically refined using the Refine All function of the software. Fluorescence signal data was added to the cells in Oufti. The resulting cell lists were processed using the MATLAB script addMeshtoCellList.m (see Supplementary Data for the code). This script uses the functions CL_getframe.m, CL_removeCell.m, CL_cellId2PositionInFrame.m, and getextradata.m which were previously described (33). Single cell fluorescence intensity values were calculated by dividing the total fluorescence signal inside a cell mesh by the cell mesh area using the MATLAB-based function CalculateFluorPerCell.m. Final fluorescence data were plotted using the GraphPad Prism 5 software. The number of cells analysed for each condition is provided in the Supplementary Data.

RESULTS

A wide palette of fluorescent proteins for imaging in *B. burgdorferi*

Only a few fluorescent proteins have been used to date in *B. burgdorferi* (summarized in Table 3). These proteins belong primarily to two colour classes: green fluorescent proteins (GFP) and red fluorescent proteins (RFP) (Table 3). To expand the range of options for multi-colour imaging of *B. burgdorferi*, we focused on a set of fluorescent proteins that have been used in localization studies in other organisms and codon-optimised their genes for translation in *B. burgdorferi*. The selected proteins span five colour classes (Table 3) and their signal can be collected using widely available filter sets for cyan fluorescent protein (CFP), GFP, yellow fluorescent protein (YFP), mCherry/TexasRed and Cy5.5 fluorescence. The selected cyan, green, and yellow variants are all derivatives of the jellyfish (*Aequorea victoria)* GFP. We used both the classic variants Cerulean (34), enhanced GFP, or EGFP (35), Citrine (36), as well as the superfolder (e.g., sfGFP) variants (37). All variants included the monomeric mutation A206K (38), denoted by a lower case m before the name of the protein (e.g., mCerulean). Our red protein of choice was mCherry (39), a monomeric, improved variant of mRFP1. Lastly, we codon-optimised and expressed an infrared fluorescent protein, iRFP (40). The far-red wavelengths used to excite this fluorophore are less toxic to cells than the shorter excitation wavelengths used for the other fluorescent proteins, and the sample autofluorescence in the near-infrared spectral region is lower than in the other, blue-shifted imaging windows (20,41).

To visualize these fluorescent proteins, we expressed them in strain B31 e2 from the strong flagellin promoter P_{flaB} (42) located on a shuttle vector. With the exception of iRFP, each fluorescent protein displayed bright fluorescence when imaged using a filter set matched to its colour (Figure 1A). Unlike the other fluorescent proteins, which oxidatively conjugate their own amino acid side chains to create a fluorophore (20), iRFP covalently binds an exogenous biliverdin molecule, which then serves as the fluorophore (40). Adding the biliverdin cofactor to the growth medium of the iRFP-expressing strain rendered the cells fluorescent in the near-infrared region of the spectrum, as detected with a Cy5.5 filter set (Figure 1B). Treating a control strain carrying an empty shuttle vector with biliverdin did not cause any increase in cellular fluorescence (data not shown). To measure cellular fluorescence levels, we chose a microscopy-based approach in conjunction with quantitative image analysis. This allowed us to efficiently analyse hundreds of cells and to clearly distinguish individual cells from similarly-sized debris found in the culture medium, or from clumps of multiple cells. Using this method, we established that a 4 μM concentration of biliverdin in the growth medium was sufficient to achieve maximal cellular brightness (Figure 1C). Close-to-maximal iRFP brightness was reached as early as an hour after addition of biliverdin to the culture and was maintained throughout subsequent growth (Figure 1D). Furthermore, continuous growth of *B. burgdorferi* in the presence of biliverdin was indistinguishable from growth in biliverdin-free medium (Figure 1E). This indicates that culture experiments that involve iRFP may be performed either by adding biliverdin shortly before imaging or by growing the cells continuously in the presence of biliverdin.

In microscopy studies, simultaneous imaging of multiple fluorescent proteins requires that the signal generated by a given fluorescent protein does not overlap with the fluorescence channels used to collect the signal of another protein. To assess the viability of using our palette of fluorescent proteins for multi-colour imaging in *B. burgdorferi*, we quantified the signal generated by each fluorescent protein when imaged with the commonly used CFP, GFP, YFP, mCherry, and Cy5.5 filter cubes (Figure 2). We found that each fluorescent protein generated a strong signal when imaged with a colour-matched filter set (Figure 2). As expected, we detected a significant spectral overlap between CFP and GFP, as well as between GFP and YFP variants. Importantly, signal quantification showed that mCerulean or msfCFP can be imaged alongside mCitrine, mCherry, and iRFP, while mEGFP or msfGFP can be imaged alongside mCherry and iRFP, opening the door to combinatorial imaging of up to four proteins in the same *B. burgdorferi* cell.

Promoters for various levels of constitutive expression in *B. burgdorferi.*

To date, constitutive expression of exogenous genes in *B. burgdorferi*, including antibiotic selection markers and reporter genes such as fluorescent proteins and luciferases, has almost exclusively relied on very strong promoters such as P_{flaB} and P_{flgB} (13,42). Reporter expression from strong promoters facilitates spirochete detection, particularly in high fluorescence background environments such as the tick midgut or mammalian tissues (43-45). However, as overexpression can affect protein localization, interfere with function, or cause cellular toxicity (e.g. (46-56)), low gene expression has proven instrumental in facilitating localization studies (e.g. (57-60)) and is often preferred in such applications.

To identify constitutively expressed promoters of low and medium strengths, we mined a published RNA sequencing (RNA-seq) dataset that measured transcript levels in cultures of *B. burgdorferi* in early-exponential, mid-exponential and stationary phases (61). We selected five genes whose expression was largely unchanged among the three growth phases tested (Figure 3A), amplified a DNA region upstream of each gene's translational start site, and fused it to an mCherry reporter in a kanamycin-resistant shuttle vector (Figure 3B). The amplified putative promoter sequences ranged in size between 129 and 212 base pairs (bp) and included the reported 5' untranslated regions (5'UTR) of these *B. burgdorferi* genes (61,62). We also included in our analysis an empty vector and a vector containing a P_{flaB}-$mCherry^{Bb}$ fusion, which served as references for no and high expression, respectively.

We transformed these constructs into *B. burgdorferi*, imaged the resulting strains, and quantified the fluorescence level in each cell. All promoters elicited fluorescence levels above the background of the strain carrying the empty vector (Figure 3C). We noticed differences between the RNA-seq and mCherry reporter methods of measuring promoter strength, as detailed in the discussion. Importantly, however, the promoters we tested displayed a broad dynamic range from low (P_{0526}) to intermediate (P_{0826}, P_{resT}, P_{0031}, and P_{0026}) to high (P_{flaB}) strength.

Antibiotic selection in *B. burgdorferi* using hygromycin B and blasticidin S resistance markers

Several antibiotic resistance markers have been used to perform genetic manipulations in *B. burgdorferi* and have recently been reviewed in detail (13). The most widely used today are the kanamycin (*aphI*), gentamicin (*aacC1*), streptomycin (*aadA*) and erythromycin (*ermC*) resistance genes (see Table 4) (42,63-65). Use of several other antibiotics for selection is either ineffective (e.g. zeocin, chloramphenicol, and puromycin), discouraged due to safety concerns (e.g. tetracyclines, β-lactams, and sometimes erythromycin), redundant due to cross-resistance (several aminoglycoside antibiotics), or no

longer widespread (coumermycin A_1) due to alterations in cell physiology induced by both the antibiotic and the resistance marker (13,64).

To expand the panel of antibiotic resistance markers that can be used in *B. burgdorferi*, we focused on two antibiotics commonly used for selection of eukaryotic cells, namely the translation inhibitors hygromycin B and blasticidin S. Rendering *B. burgdorferi* resistant to them does not pose a biosafety concern, as these antibiotics are not used to treat Lyme disease. We found that hygromycin B and blasticidin S prevented *B. burgdorferi* growth in liquid culture at concentrations of 200 and 5 μg/mL, respectively (Table 4). For resistance cassettes, we used the *E. coli* gene *hph* (also known as *aph(4)-Ia*), which encodes a hygromycin B phosphotransferase, and the *Aspergillus terreus* gene *bsd*, which encodes a blasticidin S deaminase (66-68). We codon-optimised these genes for translation in *B. burgdorferi* and placed them under the control of the strong P_{flgB} promoter on a shuttle vector (Figure 4A). The resulting vectors, pBSV2H and pBSV2B, also carry the rifampicin resistance gene *arr-2* of *Pseudomonas aeruginosa* (69-71), which encodes a rifampicin ADP-ribosyltransferase. *B. burgdorferi* is naturally resistant to rifampicin (72,73), but the use of rifampicin for selection in *E. coli* instead of the more expensive blasticidin S and hygromycin B antibiotics reduces the cost of generating and propagating the vectors in *E. coli*.

B. burgdorferi strains obtained by transforming pBSV2B or pBSV2H into B31 e2 grew readily in cultures containing 10 μg/mL blasticidin S or 250 μg/mL hygromycin B, respectively. We used these strains to test whether the antibiotic resistance cassettes encoded by these vectors conferred any cross-resistance to the often-used antibiotics kanamycin, gentamicin, streptomycin, and erythromycin. In parallel, we performed reciprocal tests using B31 e2-derived strains that carried a kanamycin, gentamicin, or streptomycin resistance cassette. Each culture was grown in the presence of two-fold serial dilutions of each antibiotic (Figure 4B). Each dilution series was centred on the concentration routinely used for selection with each of the tested antibiotics (Figure 4B, arrow). We grew the cultures for at least four days and then inspected each well for growth by dark-field imaging. A well was considered to be growth-positive if we detected at least one motile spirochete after scanning a minimum of five fields of view. In addition, we further incubated the plates to allow for growth-dependent acidification of the medium. This pH change is easily detected as a medium colour change from red, denoting no growth, to orange or yellow, denoting various degrees of growth (Figure 4C-H) (64). We confirmed that wells with the lowest antibiotic concentration at which the medium remained red also did not contain motile spirochetes. This concentration was taken to represent the minimum inhibitory concentration, or MIC (Figure 4C, black line). Whenever we exposed a strain to the antibiotic to which

it carried a resistance gene, we readily detected growth at all antibiotic concentrations tested (Figure 4D-H), highlighting the efficacy of each resistance marker. Importantly, we did not detect any major cross-resistance between the five resistance markers and the six antibiotics tested (Figure 4D-H). One exception was the kanamycin-resistant strain CJW_Bb069, which was able to grow in the presence of as much as 40 μg/mL gentamicin (Figure 4E), a concentration routinely used for gentamicin selection (64). A slightly higher amount of gentamicin (80 μg/mL) was, however, sufficient to kill this kanamycin-resistant strain (Figure 4E). This low level of cross-resistance may thus necessitate use of a higher dose of gentamicin for selection if the parental strain is already kanamycin-resistant.

DISCUSSION

We have undertaken this work to facilitate microscopy-based investigations of the biology of the Lyme disease agent *B. burgdorferi*. We expanded the available molecular toolkit by characterizing antibiotic resistance markers, fluorescent proteins and constitutively active promoters not previously used in this organism.

Alongside the commonly used kanamycin, gentamicin, streptomycin, and erythromycin selection markers, the addition of hygromycin B and blasticidin S resistances as useful selection markers will provide more flexibility in designing genetic modifications. A wider array of non-cross-resistant selection markers is particularly important in the absence of a streamlined method to create unmarked genetic modifications in this bacterium (13). Currently, in infectious *B. burgdorferi* strains, an antibiotic resistance marker is commonly used to inactivate the restriction modification system encoded by the *bbe02* locus on plasmid lp25. This inactivation increases the efficiency of transformation with shuttle vectors. It also helps maintain this plasmid in the cell population during *in vitro* growth through selective pressure (74-77). This step is essential for maintaining a strain's infectivity, as linear plasmid lp25 is essential *in vivo* but is often rapidly lost during genetic manipulations and growth in culture (78,79). A second resistance marker is often used to inactivate a gene of interest, either by targeted deletion or by transposon insertion mutagenesis. A third resistance marker is needed for complementation, either at the original locus, or *in trans*. Additional markers are needed if two genes are to be inactivated and complemented simultaneously, or if several localization reporters need to be expressed both simultaneously and independently.

Today's cell biology investigations often rely on microscopy studies using fluorescent protein fusions. Prior to our work, green and red fluorescent proteins have been the reporters of choice in *B. burgdorferi* microscopy studies (Table 3), and only a handful of subcellular localization and topology studies had

been performed using these tools (13-19). We have expanded the palette of fluorescent proteins that can be used in this bacterium by adding several proteins with properties highly desirable for imaging and localization studies. These fluorescent proteins are among the brightest of their classes (20,37,40), and their spectral properties render them appropriate for simultaneous multi-colour imaging of up to four targets. For the most part, they are also monomeric, as all of the *A. victoria* GFP, CFP, and YFP variants that we have generated carry the A206K mutation (38). Using monomeric fluorescent proteins may be important to prevent artifactual intermolecular interactions, (e.g. (38,80,81)). Should the weakly dimeric versions of these proteins be required for specific applications, the A206K mutation can be easily reversed by site-directed mutagenesis. The superfolder variants of these proteins may facilitate tagging when the folding of the fusion protein is otherwise impaired (37). In addition, unlike EGFP, which does not fold in the periplasm of diderm bacteria when exported through the Sec protein translocation system, sfGFP does fold in the periplasm (82). It can therefore be an alternative to mRFP1 and mCherry for tagging periplasmic and outer-surface-exposed proteins. This is particularly relevant for the study of *B. burgdorferi* since this bacterium expresses an unusually large number of lipoproteins that are localized on the cell surface or in the periplasmic space (83). In addition, although dimeric, iRFP may serve as a useful *in vivo* marker, and may be preferable to GFP and RFP. Excitation light penetrance in live tissues is better in the far-red/near-infrared region of the spectrum than in the blue-shifted regions used to excite GFP or RFP. Furthermore, tissue autofluorescence in this spectral region is lower, which further facilitates imaging (84,85). Lastly, the levels of biliverdin found in animal tissues are in the low milimolar range, with healthy human plasma containing 0.9-6.5 μM biliverdin (86). In our hands, such biliverdin levels are sufficient to elicit maximal fluorescence of *B. burgdorferi*-expressed iRFP. Furthermore, iRFP has been successfully used to label *Neisseria meningitidis* bacteria for *in vivo* imaging (87). Altogether, these considerations indicate that imaging in mice using iRFP-expressing *B. burgdorferi* should be feasible.

We also characterized promoters of low and intermediate strengths and demonstrated that variable degrees of constitutive gene expression can be easily achieved in *B. burgdorferi*. The relative order of promoter strength, as quantified using the mCherry reporter (Figure 3E), largely matched the order of the expression levels of the corresponding genes in culture (Figure 3A) (61), with the exceptions of P_{0526} and P_{0826}. While P_{0526} had an intermediate strength as measured by RNA-seq, it was the weakest when tested using our reporter system. In contrast, P_{0826} was the weakest promoter based on RNA-seq data, but displayed intermediate strength in our experiments. The differences may arise from strain differences or from our use of short DNA sequences of 129 to 212 bp, which presumably contain

minimal promoter sequences. Any native regulatory elements located further upstream of these short promoter sequences are thus absent in our reporter plasmids. Differences in expression levels may also be caused by reporter expression from circular shuttle vectors. P_{0526} and P_{0826} are natively located on the chromosome and differences in DNA topology, including supercoiling, between the chromosome and the circular plasmids are known to affect gene expression in *B. burgdorferi* (88,89). Finally, it is worth noting that while both *bb0526* and *bb0826* encode leaderless transcripts, *bb0826* has a secondary transcriptional start site located 54 bp upstream of the translational start site (62). This difference may also partly explain the observed promoter strength mismatch between the native gene and reporter fusion. Regardless of the reason for these discrepancies, these promoters will facilitate complementation and localization studies where medium and low gene expression levels may be required.

In summary, our study describes novel molecular tools that we hope will aid investigations in the Lyme disease field and spur further progress in the study of this medically important and highly unusual bacterium.

AVAILABILITY

Sequences of all the plasmids constructed in this study are available upon request. The DNA sequences of the various genes that were codon-optimised for expression in *B. burgdorferi* are provided in the Supplementary Data. The MATLAB code used to process cell fluorescence data is also provided as Supplementary Data.

ACCESSION NUMBERS

None.

SUPPLEMENTARY DATA

Supplementary Data are available in the accompanying document. It contains detailed plasmid construction methods, a list of oligonucleotide primer sequences used in this study, DNA sequences of genes that were codon-optimised for translation in *B. burgdorferi*, a record of cell numbers for each figure describing quantitative fluorescence data, MATLAB code used in this study, and supplementary references.

ACKNOWLEDGEMENT

We thank Nicholas Jannetty for help with cloning experiments and Dr. Bradley Parry for help with the computational analyses. We are also grateful to Drs. Brandon Jutras and Patricia Rosa, as well as to the

members of the Jacobs-Wagner laboratory for helpful discussions and/or critical reading of the manuscript.

FUNDING

This work was supported by the Howard Hughes Medical Institute. C.J.-W. is an Investigator of the Howard Hughes Medical Institute.

CONFLICT OF INTEREST

The authors are aware of no conflict of interest.

REFERENCES

1. Mead, P.S. (2015) Epidemiology of Lyme disease. *Infectious disease clinics of North America*, **29**, 187-210.
2. Steere, A.C., Strle, F., Wormser, G.P., Hu, L.T., Branda, J.A., Hovius, J.W., Li, X. and Mead, P.S. (2016) Lyme borreliosis. *Nature reviews. Disease primers*, **2**, 16090.
3. Holt, S.C. (1978) Anatomy and chemistry of spirochetes. *Microbiological reviews*, **42**, 114-160.
4. Kudryashev, M., Cyrklaff, M., Baumeister, W., Simon, M.M., Wallich, R. and Frischknecht, F. (2009) Comparative cryo-electron tomography of pathogenic Lyme disease spirochetes. *Molecular microbiology*, **71**, 1415-1434.
5. Hovind-Hougen, K. (1984) Ultrastructure of spirochetes isolated from Ixodes ricinus and Ixodes dammini. *The Yale journal of biology and medicine*, **57**, 543-548.
6. Jutras, B.L., Scott, M., Parry, B., Biboy, J., Gray, J., Vollmer, W. and Jacobs-Wagner, C. (2016) Lyme disease and relapsing fever Borrelia elongate through zones of peptidoglycan synthesis that mark division sites of daughter cells. *Proceedings of the National Academy of Sciences of the United States of America*, **113**, 9162-9170.
7. Charon, N.W., Cockburn, A., Li, C., Liu, J., Miller, K.A., Miller, M.R., Motaleb, M.A. and Wolgemuth, C.W. (2012) The unique paradigm of spirochete motility and chemotaxis. *Annual review of microbiology*, **66**, 349-370.
8. Motaleb, M.A., Corum, L., Bono, J.L., Elias, A.F., Rosa, P., Samuels, D.S. and Charon, N.W. (2000) Borrelia burgdorferi periplasmic flagella have both skeletal and motility functions. *Proceedings of the National Academy of Sciences of the United States of America*, **97**, 10899-10904.
9. Fraser, C.M., Casjens, S., Huang, W.M., Sutton, G.G., Clayton, R., Lathigra, R., White, O., Ketchum, K.A., Dodson, R., Hickey, E.K. *et al.* (1997) Genomic sequence of a Lyme disease spirochaete, Borrelia burgdorferi. *Nature*, **390**, 580-586.
10. Casjens, S., Palmer, N., van Vugt, R., Huang, W.M., Stevenson, B., Rosa, P., Lathigra, R., Sutton, G., Peterson, J., Dodson, R.J. *et al.* (2000) A bacterial genome in flux: the twelve linear and nine circular extrachromosomal DNAs in an infectious isolate of the Lyme disease spirochete Borrelia burgdorferi. *Molecular microbiology*, **35**, 490-516.
11. Radolf, J.D., Caimano, M.J., Stevenson, B. and Hu, L.T. (2012) Of ticks, mice and men: understanding the dual-host lifestyle of Lyme disease spirochaetes. *Nature reviews. Microbiology*, **10**, 87-99.
12. Rosa, P.A., Tilly, K. and Stewart, P.E. (2005) The burgeoning molecular genetics of the Lyme disease spirochaete. *Nature reviews. Microbiology*, **3**, 129-143.

13. Drecktrah, D. and Samuels, D.S. (September 17, 2017) Genetic Manipulation of Borrelia Spp. *Current topics in microbiology and immunology*, 10.1007/1082_2017_1051.
14. Xu, H., Raddi, G., Liu, J., Charon, N.W. and Li, C. (2011) Chemoreceptors and flagellar motors are subterminally located in close proximity at the two cell poles in spirochetes. *Journal of bacteriology*, **193**, 2652-2656.
15. Zhang, K., Liu, J., Charon, N.W. and Li, C. (2016) Hypothetical Protein BB0569 Is Essential for Chemotaxis of the Lyme Disease Spirochete Borrelia burgdorferi. *Journal of bacteriology*, **198**, 664-672.
16. Li, C., Xu, H., Zhang, K. and Liang, F.T. (2010) Inactivation of a putative flagellar motor switch protein FliG1 prevents Borrelia burgdorferi from swimming in highly viscous media and blocks its infectivity. *Molecular microbiology*, **75**, 1563-1576.
17. Schulze, R.J., Chen, S., Kumru, O.S. and Zuckert, W.R. (2010) Translocation of Borrelia burgdorferi surface lipoprotein OspA through the outer membrane requires an unfolded conformation and can initiate at the C-terminus. *Molecular microbiology*, **76**, 1266-1278.
18. Schulze, R.J. and Zuckert, W.R. (2006) Borrelia burgdorferi lipoproteins are secreted to the outer surface by default. *Molecular microbiology*, **59**, 1473-1484.
19. Kumru, O.S., Schulze, R.J., Slusser, J.G. and Zuckert, W.R. (2010) Development and validation of a FACS-based lipoprotein localization screen in the Lyme disease spirochete Borrelia burgdorferi. *BMC microbiology*, **10**, 277.
20. Chudakov, D.M., Matz, M.V., Lukyanov, S. and Lukyanov, K.A. (2010) Fluorescent proteins and their applications in imaging living cells and tissues. *Physiological reviews*, **90**, 1103-1163.
21. Wennmalm, S. and Simon, S.M. (2007) Studying individual events in biology. *Annual review of biochemistry*, **76**, 419-446.
22. Yao, Z. and Carballido-Lopez, R. (2014) Fluorescence imaging for bacterial cell biology: from localization to dynamics, from ensembles to single molecules. *Annual review of microbiology*, **68**, 459-476.
23. Jacobs, C., Domian, I.J., Maddock, J.R. and Shapiro, L. (1999) Cell cycle-dependent polar localization of an essential bacterial histidine kinase that controls DNA replication and cell division. *Cell*, **97**, 111-120.
24. Gordon, G.S., Sitnikov, D., Webb, C.D., Teleman, A., Straight, A., Losick, R., Murray, A.W. and Wright, A. (1997) Chromosome and low copy plasmid segregation in E. coli: visual evidence for distinct mechanisms. *Cell*, **90**, 1113-1121.
25. Arigoni, F., Pogliano, K., Webb, C.D., Stragier, P. and Losick, R. (1995) Localization of protein implicated in establishment of cell type to sites of asymmetric division. *Science*, **270**, 637-640.
26. Barbour, A.G. (1984) Isolation and cultivation of Lyme disease spirochetes. *The Yale journal of biology and medicine*, **57**, 521-525.
27. Zuckert, W.R. (2007) Laboratory maintenance of Borrelia burgdorferi. *Current protocols in microbiology*, **Chapter 12**, Unit 12C 11.
28. Jutras, B.L., Chenail, A.M. and Stevenson, B. (2013) Changes in bacterial growth rate govern expression of the Borrelia burgdorferi OspC and Erp infection-associated surface proteins. *Journal of bacteriology*, **195**, 757-764.
29. Samuels, D.S. (1995) Electrotransformation of the spirochete Borrelia burgdorferi. *Methods in molecular biology*, **47**, 253-259.
30. Grote, A., Hiller, K., Scheer, M., Munch, R., Nortemann, B., Hempel, D.C. and Jahn, D. (2005) JCat: a novel tool to adapt codon usage of a target gene to its potential expression host. *Nucleic acids research*, **33**, W526-531.
31. Nakamura, Y., Gojobori, T. and Ikemura, T. (2000) Codon usage tabulated from international DNA sequence databases: status for the year 2000. *Nucleic acids research*, **28**, 292.

32. Glaser, P., Sharpe, M.E., Raether, B., Perego, M., Ohlsen, K. and Errington, J. (1997) Dynamic, mitotic-like behavior of a bacterial protein required for accurate chromosome partitioning. *Genes & development*, **11**, 1160-1168.
33. Paintdakhi, A., Parry, B., Campos, M., Irnov, I., Elf, J., Surovtsev, I. and Jacobs-Wagner, C. (2016) Oufti: an integrated software package for high-accuracy, high-throughput quantitative microscopy analysis. *Molecular microbiology*, **99**, 767-777.
34. Rizzo, M.A., Springer, G.H., Granada, B. and Piston, D.W. (2004) An improved cyan fluorescent protein variant useful for FRET. *Nature biotechnology*, **22**, 445-449.
35. Yang, T.T., Cheng, L. and Kain, S.R. (1996) Optimized codon usage and chromophore mutations provide enhanced sensitivity with the green fluorescent protein. *Nucleic acids research*, **24**, 4592-4593.
36. Griesbeck, O., Baird, G.S., Campbell, R.E., Zacharias, D.A. and Tsien, R.Y. (2001) Reducing the environmental sensitivity of yellow fluorescent protein. Mechanism and applications. *The Journal of biological chemistry*, **276**, 29188-29194.
37. Pedelacq, J.D., Cabantous, S., Tran, T., Terwilliger, T.C. and Waldo, G.S. (2006) Engineering and characterization of a superfolder green fluorescent protein. *Nature biotechnology*, **24**, 79-88.
38. Zacharias, D.A., Violin, J.D., Newton, A.C. and Tsien, R.Y. (2002) Partitioning of lipid-modified monomeric GFPs into membrane microdomains of live cells. *Science*, **296**, 913-916.
39.Shaner, N.C., Campbell, R.E., Steinbach, P.A., Giepmans, B.N., Palmer, A.E. and Tsien, R.Y. (2004) Improved monomeric red, orange and yellow fluorescent proteins derived from Discosoma sp. red fluorescent protein. *Nature biotechnology*, **22**, 1567-1572.
40. Filonov, G.S., Piatkevich, K.D., Ting, L.M., Zhang, J., Kim, K. and Verkhusha, V.V. (2011) Bright and stable near-infrared fluorescent protein for in vivo imaging. *Nature biotechnology*, **29**, 757-761.
41. Rodriguez, E.A., Campbell, R.E., Lin, J.Y., Lin, M.Z., Miyawaki, A., Palmer, A.E., Shu, X., Zhang, J. and Tsien, R.Y. (2017) The Growing and Glowing Toolbox of Fluorescent and Photoactive Proteins. *Trends in biochemical sciences*, **42**, 111-129.
42. Bono, J.L., Elias, A.F., Kupko, J.J., 3rd, Stevenson, B., Tilly, K. and Rosa, P. (2000) Efficient targeted mutagenesis in Borrelia burgdorferi. *Journal of bacteriology*, **182**, 2445-2452.
43. Dunham-Ems, S.M., Caimano, M.J., Pal, U., Wolgemuth, C.W., Eggers, C.H., Balic, A. and Radolf, J.D. (2009) Live imaging reveals a biphasic mode of dissemination of Borrelia burgdorferi within ticks. *The Journal of clinical investigation*, **119**, 3652-3665.
44. Moriarty, T.J., Norman, M.U., Colarusso, P., Bankhead, T., Kubes, P. and Chaconas, G. (2008) Real-time high resolution 3D imaging of the lyme disease spirochete adhering to and escaping from the vasculature of a living host. *PLoS pathogens*, **4**, e1000090.
45. Hyde, J.A., Weening, E.H., Chang, M., Trzeciakowski, J.P., Hook, M., Cirillo, J.D. and Skare, J.T. (2011) Bioluminescent imaging of Borrelia burgdorferi in vivo demonstrates that the fibronectin-binding protein BBK32 is required for optimal infectivity. *Molecular microbiology*, **82**, 99-113.
46. Lybarger, S.R., Johnson, T.L., Gray, M.D., Sikora, A.E. and Sandkvist, M. (2009) Docking and assembly of the type II secretion complex of Vibrio cholerae. *Journal of bacteriology*, **191**, 3149-3161.
47. Montero Llopis, P., Jackson, A.F., Sliusarenko, O., Surovtsev, I., Heinritz, J., Emonet, T. and Jacobs-Wagner, C. (2010) Spatial organization of the flow of genetic information in bacteria. *Nature*, **466**, 77-81.
48. von Schwedler, U.K., Stuchell, M., Muller, B., Ward, D.M., Chung, H.Y., Morita, E., Wang, H.E., Davis, T., He, G.P., Cimbora, D.M. *et al.* (2003) The protein network of HIV budding. *Cell*, **114**, 701-713.
49. Zamborlini, A., Usami, Y., Radoshitzky, S.R., Popova, E., Palu, G. and Gottlinger, H. (2006) Release of autoinhibition converts ESCRT-III components into potent inhibitors of HIV-1 budding. *Proceedings of the National Academy of Sciences of the United States of America*, **103**, 19140-19145.

50. Goila-Gaur, R., Demirov, D.G., Orenstein, J.M., Ono, A. and Freed, E.O. (2003) Defects in human immunodeficiency virus budding and endosomal sorting induced by TSG101 overexpression. *Journal of virology*, **77**, 6507-6519.
51. Strack, B., Calistri, A., Craig, S., Popova, E. and Gottlinger, H.G. (2003) AIP1/ALIX is a binding partner for HIV-1 p6 and EIAV p9 functioning in virus budding. *Cell*, **114**, 689-699.
52. Martin-Serrano, J., Yarovoy, A., Perez-Caballero, D. and Bieniasz, P.D. (2003) Divergent retroviral late-budding domains recruit vacuolar protein sorting factors by using alternative adaptor proteins. *Proceedings of the National Academy of Sciences of the United States of America*, **100**, 12414-12419.
53. Lin, Y., Kimpler, L.A., Naismith, T.V., Lauer, J.M. and Hanson, P.I. (2005) Interaction of the mammalian endosomal sorting complex required for transport (ESCRT) III protein hSnf7-1 with itself, membranes, and the AAA+ ATPase SKD1. *The Journal of biological chemistry*, **280**, 12799-12809.
54. Howard, T.L., Stauffer, D.R., Degnin, C.R. and Hollenberg, S.M. (2001) CHMP1 functions as a member of a newly defined family of vesicle trafficking proteins. *Journal of cell science*, **114**, 2395-2404.
55. Broder, D.H. and Pogliano, K. (2006) Forespore engulfment mediated by a ratchet-like mechanism. *Cell*, **126**, 917-928.
56. Gregory, J.A., Becker, E.C. and Pogliano, K. (2008) Bacillus subtilis MinC destabilizes FtsZ-rings at new cell poles and contributes to the timing of cell division. *Genes & development*, **22**, 3475-3488.
57. Jouvenet, N., Simon, S.M. and Bieniasz, P.D. (2009) Imaging the interaction of HIV-1 genomes and Gag during assembly of individual viral particles. *Proceedings of the National Academy of Sciences of the United States of America*, **106**, 19114-19119.
58. Jouvenet, N., Zhadina, M., Bieniasz, P.D. and Simon, S.M. (2011) Dynamics of ESCRT protein recruitment during retroviral assembly. *Nature cell biology*, **13**, 394-401.
59. Bleck, M., Itano, M.S., Johnson, D.S., Thomas, V.K., North, A.J., Bieniasz, P.D. and Simon, S.M. (2014) Temporal and spatial organization of ESCRT protein recruitment during HIV-1 budding. *Proceedings of the National Academy of Sciences of the United States of America*, **111**, 12211-12216.
60. Itano, M.S., Bleck, M., Johnson, D.S. and Simon, S.M. (2016) Readily Accessible Multiplane Microscopy: 3D Tracking the HIV-1 Genome in Living Cells. *Traffic*, **17**, 179-186.
61. Arnold, W.K., Savage, C.R., Brissette, C.A., Seshu, J., Livny, J. and Stevenson, B. (2016) RNA-Seq of Borrelia burgdorferi in Multiple Phases of Growth Reveals Insights into the Dynamics of Gene Expression, Transcriptome Architecture, and Noncoding RNAs. *PloS one*, **11**, e0164165.
62. Adams, P.P., Flores Avile, C., Popitsch, N., Bilusic, I., Schroeder, R., Lybecker, M. and Jewett, M.W. (2017) In vivo expression technology and 5' end mapping of the Borrelia burgdorferi transcriptome identify novel RNAs expressed during mammalian infection. *Nucleic acids research*, **45**, 775-792.
63. Frank, K.L., Bundle, S.F., Kresge, M.E., Eggers, C.H. and Samuels, D.S. (2003) aadA confers streptomycin resistance in Borrelia burgdorferi. *Journal of bacteriology*, **185**, 6723-6727.
64. Elias, A.F., Bono, J.L., Kupko, J.J., 3rd, Stewart, P.E., Krum, J.G. and Rosa, P.A. (2003) New antibiotic resistance cassettes suitable for genetic studies in Borrelia burgdorferi. *Journal of molecular microbiology and biotechnology*, **6**, 29-40.
65. Sartakova, M., Dobrikova, E. and Cabello, F.C. (2000) Development of an extrachromosomal cloning vector system for use in Borrelia burgdorferi. *Proceedings of the National Academy of Sciences of the United States of America*, **97**, 4850-4855.
66. Kimura, M., Kamakura, T., Tao, Q.Z., Kaneko, I. and Yamaguchi, I. (1994) Cloning of the blasticidin S deaminase gene (BSD) from Aspergillus terreus and its use as a selectable marker for Schizosaccharomyces pombe and Pyricularia oryzae. *Molecular & general genetics : MGG*, **242**, 121-129.

67. Gritz, L. and Davies, J. (1983) Plasmid-encoded hygromycin B resistance: the sequence of hygromycin B phosphotransferase gene and its expression in Escherichia coli and Saccharomyces cerevisiae. *Gene*, **25**, 179-188.
68. Rao, R.N., Allen, N.E., Hobbs, J.N., Jr., Alborn, W.E., Jr., Kirst, H.A. and Paschal, J.W. (1983) Genetic and enzymatic basis of hygromycin B resistance in Escherichia coli. *Antimicrobial agents and chemotherapy*, **24**, 689-695.
69. Thanbichler, M., Iniesta, A.A. and Shapiro, L. (2007) A comprehensive set of plasmids for vanillate- and xylose-inducible gene expression in Caulobacter crescentus. *Nucleic acids research*, **35**, e137.
70. Qin, A., Tucker, A.M., Hines, A. and Wood, D.O. (2004) Transposon mutagenesis of the obligate intracellular pathogen Rickettsia prowazekii. *Applied and environmental microbiology*, **70**, 2816-2822.
71. Tribuddharat, C. and Fennewald, M. (1999) Integron-mediated rifampin resistance in Pseudomonas aeruginosa. *Antimicrobial agents and chemotherapy*, **43**, 960-962.
72. Johnson, S.E., Klein, G.C., Schmid, G.P. and Feeley, J.C. (1984) Susceptibility of the Lyme disease spirochete to seven antimicrobial agents. *The Yale journal of biology and medicine*, **57**, 549-553.
73. Alekshun, M., Kashlev, M. and Schwartz, I. (1997) Molecular cloning and characterization of Borrelia burgdorferi rpoB. *Gene*, **186**, 227-235.
74. Chan, K., Alter, L., Barthold, S.W. and Parveen, N. (2015) Disruption of bbe02 by Insertion of a Luciferase Gene Increases Transformation Efficiency of Borrelia burgdorferi and Allows Live Imaging in Lyme Disease Susceptible C3H Mice. *PloS one*, **10**, e0129532.
75. Rego, R.O., Bestor, A. and Rosa, P.A. (2011) Defining the plasmid-borne restriction-modification systems of the Lyme disease spirochete Borrelia burgdorferi. *Journal of bacteriology*, **193**, 1161-1171.
76. Kawabata, H., Norris, S.J. and Watanabe, H. (2004) BBE02 disruption mutants of Borrelia burgdorferi B31 have a highly transformable, infectious phenotype. *Infection and immunity*, **72**, 7147-7154.
77. Lawrenz, M.B., Kawabata, H., Purser, J.E. and Norris, S.J. (2002) Decreased electroporation efficiency in Borrelia burgdorferi containing linear plasmids lp25 and lp56: impact on transformation of infectious B. burgdorferi. *Infection and immunity*, **70**, 4798-4804.
78. Purser, J.E. and Norris, S.J. (2000) Correlation between plasmid content and infectivity in Borrelia burgdorferi. *Proceedings of the National Academy of Sciences of the United States of America*, **97**, 13865-13870.
79. Labandeira-Rey, M. and Skare, J.T. (2001) Decreased infectivity in Borrelia burgdorferi strain B31 is associated with loss of linear plasmid 25 or 28-1. *Infection and immunity*, **69**, 446-455.
80. Landgraf, D., Okumus, B., Chien, P., Baker, T.A. and Paulsson, J. (2012) Segregation of molecules at cell division reveals native protein localization. *Nature methods*, **9**, 480-482.
81. Wang, S., Moffitt, J.R., Dempsey, G.T., Xie, X.S. and Zhuang, X. (2014) Characterization and development of photoactivatable fluorescent proteins for single-molecule-based superresolution imaging. *Proceedings of the National Academy of Sciences of the United States of America*, **111**, 8452-8457.
82. Dinh, T. and Bernhardt, T.G. (2011) Using superfolder green fluorescent protein for periplasmic protein localization studies. *Journal of bacteriology*, **193**, 4984-4987.
83. Dowdell, A.S., Murphy, M.D., Azodi, C., Swanson, S.K., Florens, L., Chen, S. and Zuckert, W.R. (2017) Comprehensive Spatial Analysis of the Borrelia burgdorferi Lipoproteome Reveals a Compartmentalization Bias toward the Bacterial Surface. *Journal of bacteriology*, **199**, e00658-00616.
84. Weissleder, R. and Ntziachristos, V. (2003) Shedding light onto live molecular targets. *Nature medicine*, **9**, 123-128.

85. Jobsis, F.F. (1977) Noninvasive, infrared monitoring of cerebral and myocardial oxygen sufficiency and circulatory parameters. *Science*, **198**, 1264-1267.
86. Gafvels, M., Holmstrom, P., Somell, A., Sjovall, F., Svensson, J.O., Stahle, L., Broome, U. and Stal, P. (2009) A novel mutation in the biliverdin reductase-A gene combined with liver cirrhosis results in hyperbiliverdinaemia (green jaundice). *Liver international : official journal of the International Association for the Study of the Liver*, **29**, 1116-1124.
87. Bonazzi, D., Lo Schiavo, V., Machata, S., Djafer-Cherif, I., Nivoit, P., Manriquez, V., Tanimoto, H., Husson, J., Henry, N., Chate, H. *et al.* (May 15, 2018) Intermittent Pili-Mediated Forces Fluidize Neisseria meningitidis Aggregates Promoting Vascular Colonization. *Cell*, 10.1016/j.cell.2018.1004.1010.
88. Alverson, J., Bundle, S.F., Sohaskey, C.D., Lybecker, M.C. and Samuels, D.S. (2003) Transcriptional regulation of the ospAB and ospC promoters from Borrelia burgdorferi. *Molecular microbiology*, **48**, 1665-1677.
89. Alverson, J. and Samuels, D.S. (2002) groEL expression in gyrB mutants of Borrelia burgdorferi. *Journal of bacteriology*, **184**, 6069-6072.
90. Elias, A.F., Stewart, P.E., Grimm, D., Caimano, M.J., Eggers, C.H., Tilly, K., Bono, J.L., Akins, D.R., Radolf, J.D., Schwan, T.G. *et al.* (2002) Clonal polymorphism of Borrelia burgdorferi strain B31 MI: implications for mutagenesis in an infectious strain background. *Infection and immunity*, **70**, 2139-2150.
91. Casjens, S., van Vugt, R., Tilly, K., Rosa, P.A. and Stevenson, B. (1997) Homology throughout the multiple 32-kilobase circular plasmids present in Lyme disease spirochetes. *Journal of bacteriology*, **179**, 217-227.
92. Babb, K., McAlister, J.D., Miller, J.C. and Stevenson, B. (2004) Molecular characterization of Borrelia burgdorferi erp promoter/operator elements. *Journal of bacteriology*, **186**, 2745-2756.
93. Stewart, P.E., Thalken, R., Bono, J.L. and Rosa, P. (2001) Isolation of a circular plasmid region sufficient for autonomous replication and transformation of infectious Borrelia burgdorferi. *Molecular microbiology*, **39**, 714-721.
94. Miller, W.G., Bates, A.H., Horn, S.T., Brandl, M.T., Wachtel, M.R. and Mandrell, R.E. (2000) Detection on surfaces and in Caco-2 cells of Campylobacter jejuni cells transformed with new gfp, yfp, and cfp marker plasmids. *Applied and environmental microbiology*, **66**, 5426-5436.
95. Eggers, C.H., Caimano, M.J., Clawson, M.L., Miller, W.G., Samuels, D.S. and Radolf, J.D. (2002) Identification of loci critical for replication and compatibility of a Borrelia burgdorferi cp32 plasmid and use of a cp32-based shuttle vector for the expression of fluorescent reporters in the lyme disease spirochaete. *Molecular microbiology*, **43**, 281-295.
96. Cormack, B.P., Valdivia, R.H. and Falkow, S. (1996) FACS-optimized mutants of the green fluorescent protein (GFP). *Gene*, **173**, 33-38.
97. Miller, W.G., Leveau, J.H. and Lindow, S.E. (2000) Improved gfp and inaZ broad-host-range promoter-probe vectors. *Molecular plant-microbe interactions : MPMI*, **13**, 1243-1250.
98. Miller, W.G. and Lindow, S.E. (1997) An improved GFP cloning cassette designed for prokaryotic transcriptional fusions. *Gene*, **191**, 149-153.
99. Crameri, A., Whitehorn, E.A., Tate, E. and Stemmer, W.P. (1996) Improved green fluorescent protein by molecular evolution using DNA shuffling. *Nature biotechnology*, **14**, 315-319.
100. Carroll, J.A., Stewart, P.E., Rosa, P., Elias, A.F. and Garon, C.F. (2003) An enhanced GFP reporter system to monitor gene expression in Borrelia burgdorferi. *Microbiology*, **149**, 1819-1828.
101. Campbell, R.E., Tour, O., Palmer, A.E., Steinbach, P.A., Baird, G.S., Zacharias, D.A. and Tsien, R.Y. (2002) A monomeric red fluorescent protein. *Proceedings of the National Academy of Sciences of the United States of America*, **99**, 7877-7882.

652 102. Lee, W.Y., Moriarty, T.J., Wong, C.H., Zhou, H., Strieter, R.M., van Rooijen, N., Chaconas, G.
653 and Kubes, P. (2010) An intravascular immune response to Borrelia burgdorferi involves Kupffer
654 cells and iNKT cells. *Nature immunology*, **11**, 295-302.
655 103. Sartakova, M.L., Dobrikova, E.Y., Terekhova, D.A., Devis, R., Bugrysheva, J.V., Morozova,
656 O.V., Godfrey, H.P. and Cabello, F.C. (2003) Novel antibiotic-resistance markers in pGK12-derived
657 vectors for Borrelia burgdorferi. *Gene*, **303**, 131-137.
658 104. Terekhova, D., Sartakova, M.L., Wormser, G.P., Schwartz, I. and Cabello, F.C. (2002)
659 Erythromycin resistance in Borrelia burgdorferi. *Antimicrobial agents and chemotherapy*, **46**, 3637-
660 3640.

661

662 **FIGURES LEGENDS**

663 **Figure 1.** Fluorescent protein characterization. **A.** *B. burgdorferi* strains CJW_Bb090 through
664 CJW_Bb096 expressing the indicated fluorescent proteins were imaged with matching filter sets. **B.**
665 Strain CJW_Bb100 expressing iRFP requires biliverdin for development of fluorescence. Cells were
666 grown in liquid culture with biliverdin for two days prior to imaging using a Cy5.5 filter set. **C.** Dose-
667 response of iRFP fluorescence to biliverdin concentration. Strain CJW_Bb100 was grown in the
668 presence of biliverdin for two days prior to imaging. Between 86 and 206 cells were analysed for each
669 concentration. Total cellular fluorescence levels were normalized by the cell area. Shown are means ±
670 standard deviations (SD). A.U., arbitrary units. **D.** Time-course of iRFP fluorescence development in
671 strain CJW_Bb100 following addition of 16 μM biliverdin. Between 68 and 110 cells were analysed for
672 each time point. **E.** Biliverdin does not affect *B. burgdorferi* growth. Strain CJW_Bb100 was inoculated
673 at 10^4 cells/mL in duplicate in medium containing 4 μM biliverdin or no biliverdin, after which the
674 spirochetes were enumerated daily.

675 **Figure 2.** Quantification of fluorescent protein signal using common fluorescence filter sets. Strains
676 CJW_Bb090 through CJW_Bb096 and CJW_Bb100 expressing the fluorescent proteins indicated at the
677 bottom of the figure were each imaged using five filter sets: CFP, GFP, YFP, mCherry/TexasRed, and
678 Cy5.5 (see the Materials and Methods section for filter set specifications). Strain CJW_Bb073 carrying
679 an empty shuttle vector (EV) was also imaged to measure the cellular autofluorescence. Each filter set is
680 listed at the top of the corresponding graph. Fluorescence intensity values were normalized by the cell
681 area and are depicted as means ± SD in arbitrary units (A.U.). For each strain, 117 to 308 cells were
682 analysed. The iRFP strain was grown in the presence of 4 μM biliverdin for three days prior to imaging.
683 Coloured background highlights the data obtained with filter sets that were ideal for the expressed
684 fluorescent protein.

Figure 3. Promoter strength quantification. **A.** mRNA expression levels extracted from published RNA-seq data obtained using strain B31-A3 (90) grown to early exponential phase (10^6 cells/mL), mid-exponential phase (10^7 cells/mL), or stationary phase (one day after reaching 10^8 cells/mL) (61). FPKM, fragments per kilobase transcript per million mapped reads. **B.** Promoter reporter plasmid map (not drawn to scale). IR, inverted repeats; cp9 *ori*, origin or replication of *B. burgdorferi* plasmid cp9, which includes the genes *orf1*, *orf2*, *orf3* needed for plasmid replication in *B. burgdorferi*; colE1 *ori*, *E. coli* origin of replication; P_{flgB}, *B. burgdorferi* flagellar rod operon promoter; *aphI*, kanamycin resistance gene. The promoter (blue) and the mCherry-coding sequence (red) are connected by a BamHI restriction enzyme site and a ribosomal binding site (RBS). The native locus from which the promoter was extracted is depicted below the plasmid map. The BamHI-RBS-mCherry sequence effectively replaced the gene's protein coding sequence shown in pink. Translational START sites are marked by the ATG codon. **C.** Promoter strength quantified by measuring cellular mCherry fluorescence in strains CJW_Bb069, CJW_Bb108 through CJW_Bb112, and CJW_Bb146. The fluorescence levels were normalized by the cell area. The promoters were ranked in increasing order of the mean fluorescence values and are listed below the graph. Shown are means ± SD. Between 97 and 160 cells were analysed per strain. EV, empty vector; A.U., arbitrary units.

Figure 4. Characterization of blasticidin S and hygromycin B resistances in *B. burgdorferi*. **A.** Maps of shuttle vectors pBSV2B and pBSV2H. IR, inverted repeats; cp9 *ori*, origin or replication of *B. burgdorferi* plasmid cp9; colE1 *ori*, *E. coli* origin of replication; MCS, multicloning site; *arr-2*, rifampicin resistance gene for selection in *E. coli*; P_{flgB}, *B. burgdorferi* flagellar rod operon promoter; bsd^{Bb}, *B. burgdorferi* codon-optimised blasticidin S deaminase-encoding gene; hph^{Bb}, *B. burgdorferi* codon-optimised hygromycin B phosphotransferase-encoding gene. The maps are not drawn to scale. **B.** Plate map showing the final antibiotic concentrations used for cross-resistance testing. Each concentration was tested in two adjacent wells. Concentrations routinely used for selection are indicated by the arrow. **C.** Schematic representation of colour change of the growth medium from red (absence of spirochete growth) to orange/yellow (presence of spirochete growth). A line marks the boundary between growth and no growth in an antibiotic concentration series. The lowest antibiotic concentration that blocked growth was identified as the minimal inhibitory concentration (MIC). **D.-H.** Susceptibility test of each resistance-carrying strain to various antibiotic concentrations according to the plate layout shown in B. The plates were incubated to allow for growth-dependent acidification of the medium and change in phenol red pH indicator colour from red to orange and yellow, as depicted in panel C. Images

716 were obtained using colourimetric imaging of the individual plates. MIC boundaries are marked by dark
717 lines. The strains used are listed above each image.

718

719 **TABLES**

Table 1. Strains used in this study

Strain	Genotype / description	Antibiotic resistance	Source or reference
	***E. coli* cloning strains**		
DH5α	F$^-$ Φ80*dlacZΔM15* Δ(*lacZYA-argF*) U169 *deoR recA1 endA1 hsdR17* (r_k^-, m_k^+) *phoA supE44* λ$^-$*thi-1 gyrA96 relA1*	None	Promega
XL10-Gold	Tet^{r}Δ(*mcrA*)*183* Δ(*mcrCB-hsdSMR-mrr*)*173 endA1 supE44 thi*$^-$*1 recA1 gyrA96 relA1 lac* Hte [F´ *proAB lacI*^{q}*ZΔM15* Tn*10* (Tet^r) Amy Cam^r]	Tetracycline Chloramphenicol	Agilent
	***B. burgdorferi* strains**		
B31 MI	Low-passage derivative of the type strain B31	None	(9)
B31 e2	Reduced genome non-infectious clone of strain B31	None	(91)
CJW_Bb069	B31 e2 / pBSV2_2	Kanamycin	This study
CJW_Bb070	B31 e2 / pKFSS1_2	Streptomycin	This study
CJW_Bb071	B31 e2 / pBSV2H	Hygromycin B	This study
CJW_Bb072	B31 e2 / pBSV2B	Blasticidin S	This study
CJW_Bb073	B31 e2 / pBSV2G_2	Gentamicin	This study
CJW_Bb090	B31 e2 / pBSV2G_P_{flaB}-msfGFP^{Bb}	Gentamicin	This study
CJW_Bb091	B31 e2 / pBSV2G_P_{flaB}-msfCFP^{Bb}	Gentamicin	This study
CJW_Bb092	B31 e2 / pBSV2G_P_{flaB}-msfYFP^{Bb}	Gentamicin	This study
CJW_Bb093	B31 e2 / pBSV2G_P_{flaB}-mCherry^{Bb}	Gentamicin	This study
CJW_Bb094	B31 e2 / pBSV2G_P_{flaB}-mEGFP^{Bb}	Gentamicin	This study
CJW_Bb095	B31 e2 / pBSV2G_P_{flaB}-mCerulean^{Bb}	Gentamicin	This study
CJW_Bb096	B31 e2 / pBSV2G_P_{flaB}-mCitrine^{Bb}	Gentamicin	This study
CJW_Bb100	B31 e2 / pBSV2G_P_{flaB}-iRFP^{Bb}	Gentamicin	This study
CJW_Bb108	B31 e2 / pBSV2_P_{resT}-mCherry^{Bb}	Kanamycin	This study
CJW_Bb109	B31 e2 / pBSV2_P_{0026}-mCherry^{Bb}	Kanamycin	This study
CJW_Bb110	B31 e2 / pBSV2_P_{0031}-mCherry^{Bb}	Kanamycin	This study
CJW_Bb111	B31 e2 / pBSV2_P_{0526}-mCherry^{Bb}	Kanamycin	This study
CJW_Bb112	B31 e2 / pBSV2_P_{0826}-mCherry^{Bb}	Kanamycin	This study
CJW_Bb146	B31 e2 / pBSV2_P_{flaB}-mCherry^{Bb}	Kanamycin	This study

720

721

722

723

724

Table 2. Plasmids used in this study.

Plasmid name	Description	Antibiotic resistance	Reference
pBSV2G	Gentamicin-resistant *B. burgdorferi* shuttle vector	Gentamicin	(64)
pBLS599	pBSV2-derived *B. burgdorferi* shuttle vector lacking the zeocin gene; expresses *gfpmut3*	Kanamycin	(92)
pKFSS1	Streptomycin-resistant *B. burgdorferi* shuttle vector	Streptomycin	(63)
pMCS-3	Plasmid carrying the rifampicin resistance gene *arr-2*	Rifampicin	(69)
pSL1180	Ampicillin-resistant cloning plasmid	Ampicillin	Amersham
pBSV2G_2	Modified gentamicin-resistant *B. burgdorferi* shuttle vector; has extended multicloning site	Gentamicin	This study
pBSV2_2	Kanamycin-resistant *B. burgdorferi* shuttle vector similar to pBSV2 (93); lacks the zeocin gene; has extended multicloning site	Kanamycin	This study
pKFSS1_2	Modified streptomycin-resistant *B. burgdorferi* shuttle vector; has extended multicloning site	Streptomycin	This study
pBSV2B	Blasticidin S-resistant *B. burgdorferi* shuttle vector; uses rifampicin for selection in *E. coli*	Blasticidin S Rifampicin	This study
pBSV2H	Hygromycin B-resistant *B. burgdorferi* shuttle vector; uses rifampicin for selection in *E. coli*	Hygromycin B Rifampicin	This study
pBSV2G_P_{flaB}-mCherry^{Bb}	For expression of mCherry^{Bb} under the control of the strong *B. burgdorferi* promoter P_{flaB}	Gentamicin	This study
pBSV2G_P_{flaB}-msfGFP^{Bb}	For expression of msfGFP^{Bb} under the control of the strong *B. burgdorferi* promoter P_{flaB}	Gentamicin	This study
pBSV2G_P_{flaB}-msfCFP^{Bb}	For expression of msfCFP^{Bb} under the control of the strong *B. burgdorferi* promoter P_{flaB}	Gentamicin	This study
pBSV2G_P_{flaB}-msfYFP^{Bb}	For expression of msfYFP^{Bb} under the control of the strong *B. burgdorferi* promoter P_{flaB}	Gentamicin	This study
pBSV2G_P_{flaB}-mEGFP^{Bb}	For expression of mEGFP^{Bb} under the control of the strong *B. burgdorferi* promoter P_{flaB}	Gentamicin	This study
pBSV2G_P_{flaB}-mCerulean^{Bb}	For expression of mCerulean^{Bb} under the control of the strong *B. burgdorferi* promoter P_{flaB}	Gentamicin	This study
pBSV2G_P_{flaB}-mCitrine^{Bb}	For expression of mCitrine^{Bb} under the control of the strong *B. burgdorferi* promoter P_{flaB}	Gentamicin	This study
pBSV2G_P_{flaB}-iRFP^{Bb}	For expression of iRFP^{Bb} under the control of the strong *B. burgdorferi* promoter P_{flaB}	Gentamicin	This study
pBSV2_P_{resT}-mCherry^{Bb}	For expression of mCherry^{Bb} under the control of the *B. burgdorferi* promoter P_{resT}	Kanamycin	This study
pBSV2_P_{0026}-mCherry^{Bb}	For expression of mCherry^{Bb} under the control of the *B. burgdorferi* promoter P_{0026}	Kanamycin	This study
pBSV2_P_{0031}-mCherry^{Bb}	For expression of mCherry^{Bb} under the control of the *B. burgdorferi* promoter P_{0031}	Kanamycin	This study
pBSV2_P_{0526}-mCherry^{Bb}	For expression of mCherry^{Bb} under the control of the *B. burgdorferi* promoter P_{0526}	Kanamycin	This study
pBSV2_P_{0826}-mCherry^{Bb}	For expression of mCherry^{Bb} under the control of the *B. burgdorferi* promoter P_{0826}	Kanamycin	This study
pBSV2_P_{flaB}-mCherry^{Bb}	For expression of mCherry^{Bb} under the control of the strong *B. burgdorferi* promoter P_{flaB}	Kanamycin	This study

Table 3. Fluorescent proteins used in *B. burgdorferi*

Colour class	Protein expressed	Ex/Em[a] max (nm)	Source or reference for protein/gene development	Reference for use in *B. burgdorferi*	Notes
I. Fluorescent proteins previously used in *B. burgdorferi:*					
Cyan	CFP	434/477[b]	Clontech; (94)	(95)	Rarely used
Green	EGFP	489/509	Clontech; (35)	(65)	Low expression; has mammalian codon usage
	GFPmut1	488/507	(94,96-98)	(95)	Widely used; adapted for bacterial expression; same protein as EGFP
	GFPmut3	501/511	(96)	(92)	
	GFP cycle 3	NR[c]	(99)	(100)	Retains UV excitation peak
Yellow	YFP	514/527[b]	(94)	(95)	Rarely used
Red	mRFP1	584/607	(101)	(18)	Folds in the periplasm
	dTomato	554/581	(39)	(102)	Dimeric
II. New fluorescent proteins adapted for use in *B. burgdorferi:*					
Cyan	mCerulean	433/475	(34)	This study	A206K monomeric mutation
	msfCFP	NR[c]	(37)	This study	A206K mutation; superfolder
Green	mEGFP	489/509	(35)	This study	A206K mutation
	msfGFP	485/NR[c]	(37)	This study	A206K mutation; superfolder
Yellow	mCitrine	516/529	(36)	This study	A206K mutation
	msfYFP	NR[c]	(37)	This study	A206K mutation; superfolder
Red	mCherry	587/610	(39)	This study	
Infrared	iRFP	690/713	(40)	This study	Dimeric

[a] Maximum excitation (Ex) and emission (Em) wavelengths; [b]values assumed to be those for ECFP and EYFP, respectively (20); [c]NR, not reported: values were not reported in the original publication, or could not be exactly inferred from excitation and emission graphs.

Table 4. Summary of antibiotic resistance markers used in *B. burgdorferi*[a]

Resistance gene	Antibiotic	MIC[b] (µg/mL)	Notes	References
I. Widely used resistance markers				
aphI	Kanamycin	<25	Cross-resistance to neomycin, lividomycin, paromomycin, ribostamycin	(42,64)
aadA	Streptomycin	7[c]	Expected cross-resistance to spectinomycin	(63)
aacC1	Gentamicin	<15.6		(64)
ermC	Erythromycin	0.005	Resistance level varies among strains; May pose safety risk	(65,103,104)
II. Newly developed resistance markers				
bsd^{Bb}	Blasticidin S	<5	Neither marker provides cross-resistance to	This study
hph^{Bb}	Hygromycin B	<200	the selection antibiotics listed above.	This study

[a]For space considerations, this table does not contain a comprehensive list of antibiotic resistance markers developed for use in *B. burgdorferi*. For a detailed discussion of other markers, please see (13); [b]Minimal inhibitory concentration, determined in liquid culture; [c]Value is that of an inhibitory dose 50, or ID_{50}.

731

Figure 1

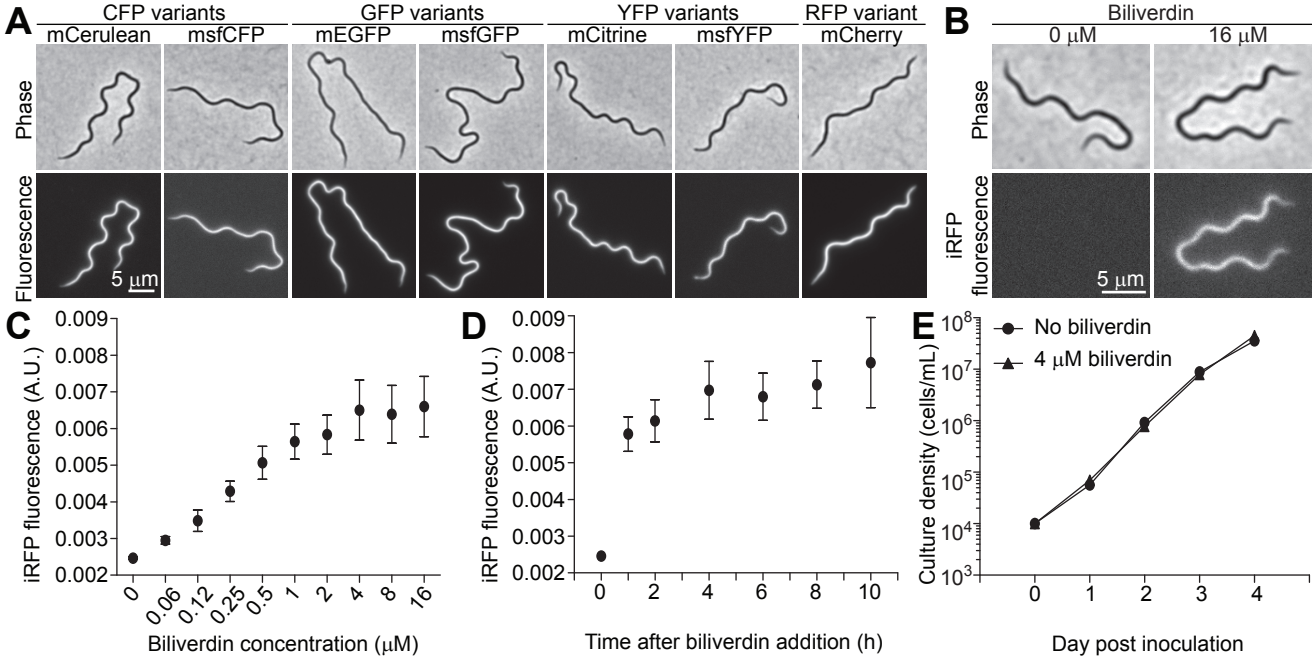
A
CFP variants
mCerulean
msfCFP
GFP variants
mEGFP
msfGFP
YFP variants
mCitrine
msfYFP
RFP variant
mCherry
Phase
Fluorescence
5 μm
B
Biliverdin
0 μM
16 μM
Phase
iRFP fluorescence
5 μm
C
iRFP fluorescence (A.U.)
0.009
0.008
0.007
0.006
0.005
0.004
0.003
0.002
0
0.06
0.12
0.25
0.5
1
2
4
8
16
Biliverdin concentration (μM)
D
iRFP fluorescence (A.U.)
0.009
0.008
0.007
0.006
0.005
0.004
0.003
0.002
0
2
4
6
8
10
Time after biliverdin addition (h)
E
No biliverdin
4 μM biliverdin
Culture density (cells/mL)
10^8
10^7
10^6
10^5
10^4
10^3
0
1
2
3
4
Day post inoculation

Figure 2

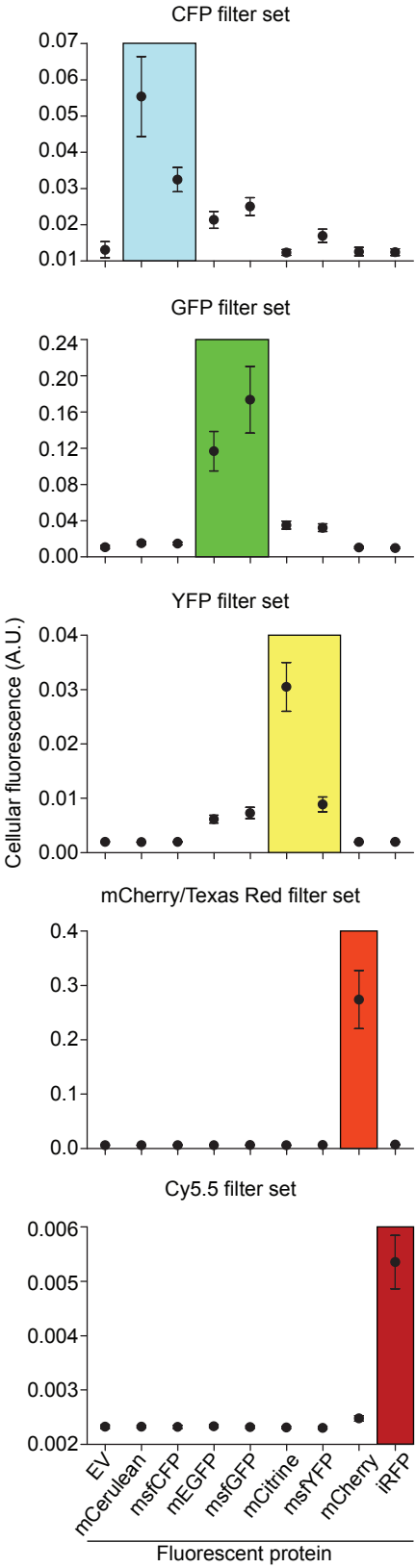
CFP filter set
0.07
0.06
0.05
0.04
0.03
0.02
0.01
GFP filter set
0.24
0.20
0.16
0.12
0.08
0.04
0.00
YFP filter set
Cellular fluorescence (A.U.)
0.04
0.03
0.02
0.01
0.00
mCherry/Texas Red filter set
0.4
0.3
0.2
0.1
0.0
Cy5.5 filter set
0.006
0.005
0.004
0.003
0.002
EV
mCerulean
msfCFP
mEGFP
msfGFP
mCitrine
msfYFP
mCherry
iRFP
Fluorescent protein

Figure 3

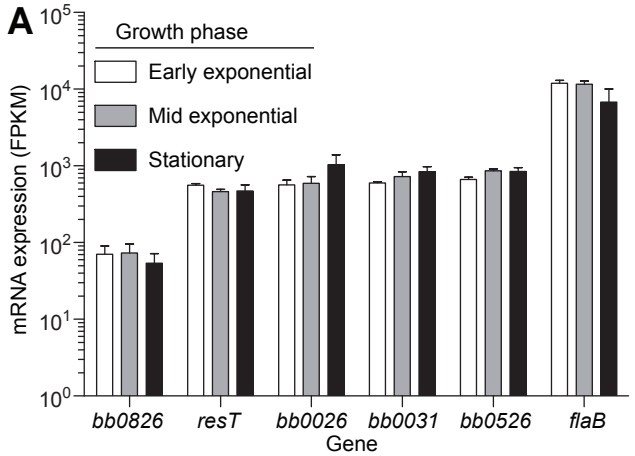
A
Growth phase
Early exponential
Mid exponential
Stationary
mRNA expression (FPKM)
bb0826
resT
bb0026
bb0031
bb0526
flaB
Gene

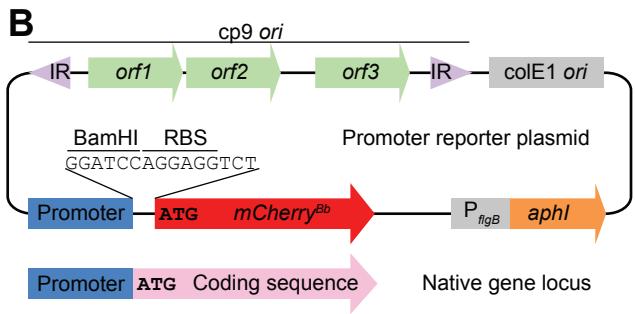
B
cp9 ori
IR
orf1
orf2
orf3
IR
colE1 ori
BamHI
RBS
GGATCCAGGAGGTCT
Promoter reporter plasmid
Promoter
ATG
mCherryBb
PflgB
aphI
Promoter
ATG
Coding sequence
Native gene locus

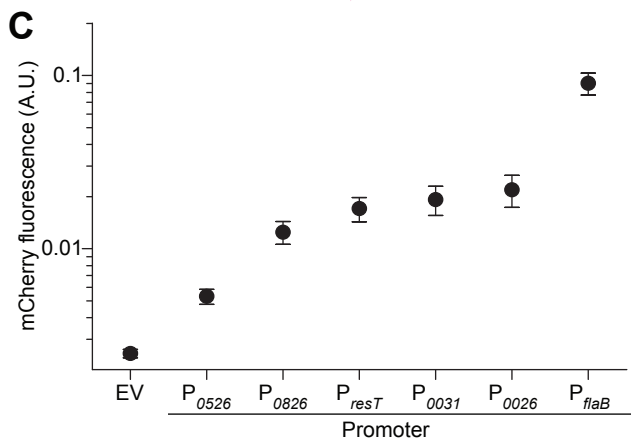
C
mCherry fluorescence (A.U.)
0.1
0.01
EV
P0526
P0826
PresT
P0031
P0026
PflaB
Promoter

Figure 4

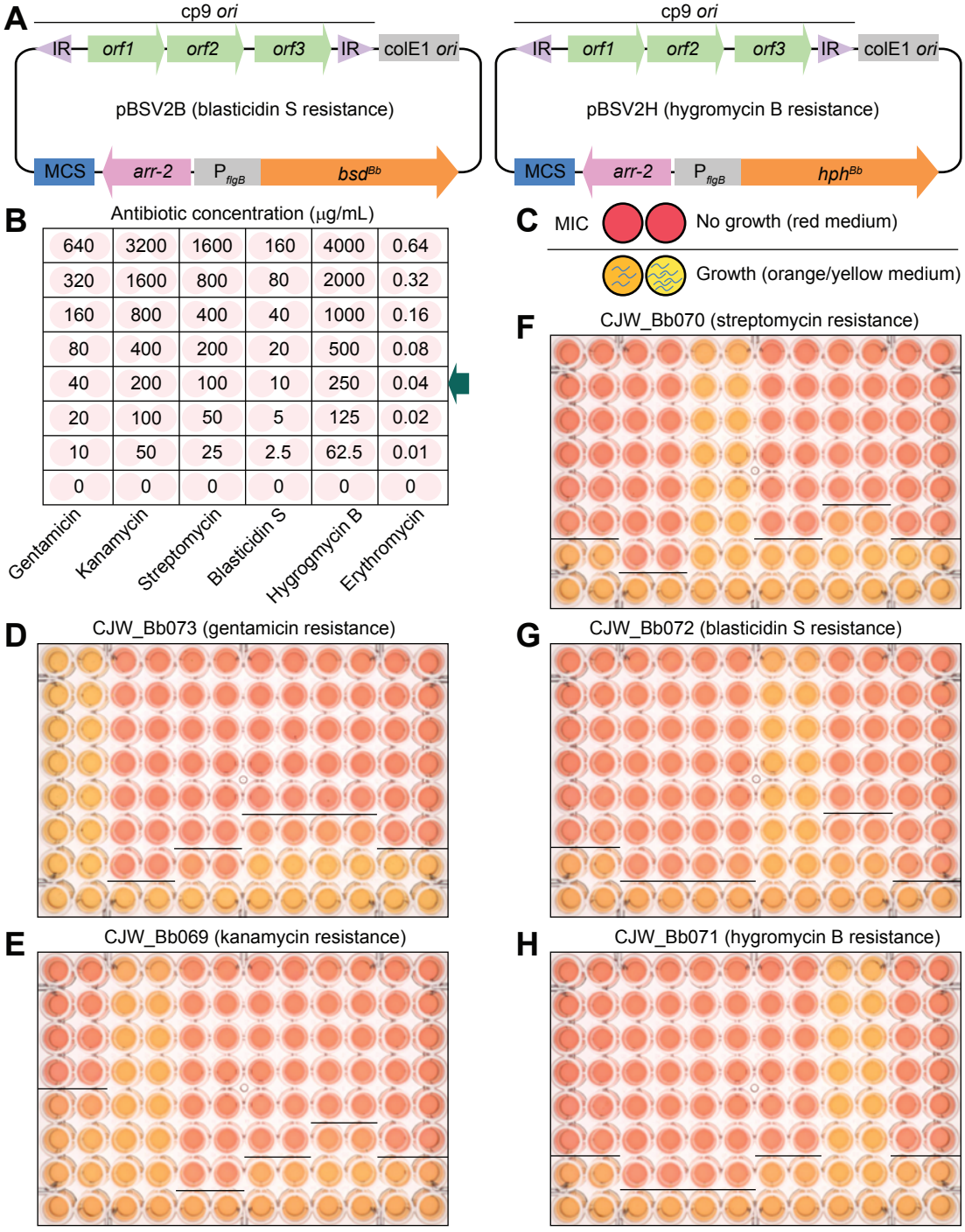
A
cp9 ori
IR
orf1
orf2
orf3
IR
colE1 ori
pBSV2B (blasticidin S resistance)
MCS
arr-2
P flgB
bsd Bb
cp9 ori
IR
orf1
orf2
orf3
IR
colE1 ori
pBSV2H (hygromycin B resistance)
MCS
arr-2
P flgB
hph Bb
B
Antibiotic concentration (μg/mL)
640 3200 1600 160 4000 0.64
320 1600 800 80 2000 0.32
160 800 400 40 1000 0.16
80 400 200 20 500 0.08
40 200 100 10 250 0.04
20 100 50 5 125 0.02
10 50 25 2.5 62.5 0.01
0 0 0 0 0 0
Gentamicin
Kanamycin
Streptomycin
Blasticidin S
Hygromycin B
Erythromycin
C
MIC
No growth (red medium)
Growth (orange/yellow medium)
D
CJW_Bb073 (gentamicin resistance)
E
CJW_Bb069 (kanamycin resistance)
F
CJW_Bb070 (streptomycin resistance)
G
CJW_Bb072 (blasticidin S resistance)
H
CJW_Bb071 (hygromycin B resistance)

Characterization of fluorescent proteins, promoters, and selectable markers for applications in the Lyme disease spirochete *Borrelia burgdorferi*.

Constantin N. Takacs, Molly Scott and Christine Jacobs-Wagner

SUPPLEMENTARY DATA

Contents:

I. Detailed plasmid construction methods.....S1

II. Supplementary Table: Oligonucleotide primer sequences.....S5

III. DNA sequences of genes codon-optimised for translation in *B. burgdorferi*.....S6

IV. Supplementary Table: Numbers of cells analysed to generate quantitative data.....S10

V. MATLAB code.....S11

VI. Supplementary references.....S15

I. Detailed plasmid construction methods

Mutagenesis, plasmid preparation, and cloning

Site-directed mutagenesis was performed using Agilent's QuickChange Lightning Site Directed Mutagenesis Kit, as per the kit's instructions. Restriction endonucleases (regular and high-fidelity versions) and Electroligase were purchased from New England Biolabs. DNA polymerases were from Thermo Scientific (Platinum PCR Supermix), New England Biolabs (Phusion), or Takara (Prime Star). Oligonucleotide primers were synthesized at Integrated DNA Technologies and are listed in the supplementary table below. Gel extraction was performed using the Purelink Quick Gel Extraction Kit (Thermo Scientific). DNA minipreps were done using Zyppy plasmid miniprep kit (Zymo Research), while midipreps were done using the Plasmid Plus Midi Kit (Qiagen) from 50 mL of overnight *Escherichia coli* cultures in Super Broth. Correct insert DNA sequences were confirmed at Quintarabio or using an in-house Sanger DNA sequencing service at the Yale Keck Biotechnology Resource Laboratory.

Expansion of the multicloning site of extant shuttle vectors. The multicloning site of the shuttle vectors kanamycin-resistant pBSV2 (1), gentamicin-resistant pBSV2G (2) and streptomycin-resistant pKFSS1 (3) was modified to facilitate cloning by including several additional restriction enzyme sites. The modified vectors were named pBSV2_2, BSV2G_2, and pKFSS1_2, respectively. The multicloning site of the original vectors contains the following restriction enzyme sites, in order: SacI-**KpnI-XmaI-BamHI**-XbaI-SalI-PstI-SphI-HindIII. The expanded multicloning site contains the following restriction enzyme sites, in order: SacI-**AgeI-XhoI-AatII-NheI-BamHI-XmaI-KpnI**-XbaI-SalI-PstI-SphI-HindIII. The regions of the multicloning site that were modified are marked in bold letters. We note that the AatII and XmaI sites are not unique in shuttle vector pKFSS1_2, and that the XhoI site is not unique in shuttle vectors pBSV2_2 and pKFSS1_2. To construct **pBSV2G_2**, the multicloning site of the shuttle vector was extended by annealing primers NT23 and NT24 and ligating the product into BamHI/KpnI-digested pBSV2G. To construct **pBSV2_2**, the SacI/BbsI fragment of pBSV2G_2 containing the extended multicloning site and part of the flagellar rod operon promoter (P_{flgB}) was cloned into the SacI/BbsI sites of pBLS599. During derivation of pBLS599 from pBSV2, the zeocin cassette of pBSV2 was removed (4). Thus, pBSV2_2 differs from pBSV2 in that it lacks the zeocin resistance cassette and has an expanded multicloning site. To construct **pKFSS1_2**, the BbsI/SacI fragment of pBSV2G_2 was moved into the BbsI/SacI sites of pKFSS1.

New shuttle vectors carrying blasticidin S and hygromycin B antibiotic resistance markers. To construct **pBSV2B**, the following three fragments were assembled in order into the cloning plasmid pSL1180: (i) the *arr-2* rifampicin resistance gene, including its promoter, was PCR amplified from plasmid pMCS-3 using primers NT169 and NT170, digested with AvrII and EagI, and inserted into the AvrII/EagI sites of pSL1180 to form pSL1180_arr2, (ii) a *B. burgdorferi* codon-optimised blasticidin S deaminase gene, bsd^{Bb}, was synthesized. It was then PCR amplified with NT171 and NT172, digested with PstI and MluI and inserted into the PstI/MluI sites of pSL1880_arr2 to form pSL1180_arr2-bsd^{Bb}, (iii) the P_{flgB} sequence of pBSV2G was amplified using NT173 and NT174, digested with EagI and NdeI and inserted into the EagI/NdeI sites of pSL1180_arr2-bsd^{Bb} to yield pSL1180_arr2-P_{flgB}-bsd^{Bb}. The resulting *arr2*-P_{flgB}-bsd^{Bb} cassette was excised using MluI and AvrII and ligated into the MluI/AvrII backbone of pBSV2G_2. To construct **pBSV2H**, a *B. burgdorferi* codon-optimised hygromycin B resistance gene, hph^{Bb}, was synthesized. This gene was moved as an NdeI/MluI fragment into the NdeI/MluI backbone of pSL1180_arr2-P_{flgB}-bsd^{Bb}, an intermediate for the construction of pBSV2B (see

above), thereby yielding pSL1180_arr2-P_{flgB}-hph^{Bb}. The resulting *arr2*- P_{flgB} -hph^{Bb} cassette was excised using MluI and AvrII and ligated into the MluI/AvrII backbone of pBSV2G_2.

Constructs for expression of fluorescent proteins from the flagellin promoter. *B. burgdorferi* codon-optimised fluorescent protein-coding genes *mCerulean*^{Bb}, *mEGFP*^{Bb}, *msfGFP*^{Bb}, *mCitrine*^{Bb}, *mCherry*^{Bb}, and *iRFP*^{Bb} were synthesized. Site-directed mutagenesis was performed on the *msfGFP*^{Bb} sequence using primer pairs NT187/NT188 or NT189/N190 to introduce the Y66W or T203Y mutations and create the *msfCFP*^{Bb} and *msfYFP*^{Bb} genes, respectively. A BamHI (GGATCC) site was included immediately upstream of the START ATG codon either during gene synthesis or during PCR amplification of the fluorescent protein-encoding genes. A HindIII site was included, overlapping with and downstream of the STOP TAA codon (as a TAAGCTT sequence, with the HindIII site underlined), either during gene synthesis or during PCR amplification. *mCherry*^{Bb} was PCR amplified using NT100 and NT193. *msfCFP*^{Bb} and *msfYFP*^{Bb} were PCR amplified using NT160 and NT161. The BamHI/HindIII site-flanked fluorescent protein-encoding genes were released from PCR products or parental plasmids using BamHI and HindIII. The flagellin promoter (P_{flaB}) sequence (5) was PCR amplified from *B. burgdorferi* genomic DNA using primers NT27 and NT28 and digested with SacI and BamHI. For each transcriptional fusion to P_{flaB}, a P_{flaB} SacI/BamHI fragment and a BamHI/HindIII fragment of the fluorescent protein-encoding gene were assembled, via intermediary constructs, into the SacI/HindIII sites of pBSV2G_2 or pBSV2_2, thus yielding **pBSV2G_P_{flaB}-mCerulean^{Bb}**, **pBSV2G_P_{flaB}-msfCFP^{Bb}**, **pBSV2G_P_{flaB}-mEGFP^{Bb}**, **pBSV2G_P_{flaB}-msfGFP^{Bb}**, **pBSV2G_P_{flaB}-mCitrine^{Bb}**, **pBSV2G_P_{flaB}-msfYFP^{Bb}**, **pBSV2G_P_{flaB}-mCherry^{Bb}**, **pBSV2G_P_{flaB}-iRFP^{Bb}**, and **pBSV2_P_{flaB}-mCherry^{Bb}**.

Promoters for mCherry^{Bb} reporter expression. Through intermediary constructs, promoter sequences were inserted between the SacI and BamHI sites of pBSV2_2, while the *mCherry*^{Bb} gene was amplified using NT193 and NT342, digested using BamHI and HindIII, and inserted into the BamHI/HindIII sites of the same pBSV2_2 backbone, resulting in kanamycin-resistant shuttle vectors carrying *mCherry*^{Bb} transcriptional fusions. The primer NT342 contains a ribosome binding site (RBS) sequence (AGGAGG) downstream of the BamHI site (GGATCC) and upstream of the ATG start codon of the mCherry-encoding gene. The full sequence is ggatccAGGAGGctcATG, with the BamHI site and a 3-nucleotide spacer sequence in lower case letters and the ribosomal binding site (RBS) and the

START codon in upper case letters. The following primers and B31 genomic DNA were used to amplify the various promoters used: NT107 and NT108 (amplify nucleotides 2187 to 2371 of the reverse strand of the B31 cp26 plasmid, GenBank accession number NC_001903) for the telomere resolvase promoter P_{resT}, NT109 and NT110 (amplify nucleotides 25623 to 25751 of the reverse strand of the B31 chromosome, GenBank accession number NC_001318_1) for P_{0026}, NT111 and NT112 (amplify nucleotides 29472 to 29669 of the reverse strand of the chromosome) for P_{0031}, NT113 and NT114 (amplify nucleotides 535523 to 535703 of the forward strand of the chromosome) for P_{0526}, NT115 and NT116 (amplify nucleotides 870024 to 870235 of the reverse strand of the chromosome) for P_{0826}. The following constructs were thus obtained: **pBSV2_ P_{resT}-mCherry^{Bb}**, **pBSV2_P_{0026}-mCherry^{Bb}**, **pBSV2_P_{0031}-mCherry^{Bb}**, **pBSV2_P_{0526}-mCherry^{Bb}**, **pBSV2_P_{0826}-mCherry^{Bb}**.

II. Supplementary Table: Oligonucleotide primer sequences

Primer name	Sequence[a] (5' to 3')
NT23	accggtctcgaggacgtcgctagcggatcccggggtacc
NT24	gatcggtaccccgggatccgctagcgacgtcctcgagaccggtgtac
NT27	tatagagctctgtctgtcgcctcttgtggcttcc
NT28	cacggatcctcattcctccatgataaaatttaaatttctgac
NT100	tatggatccatggttagtaaaggtgaagaag
NT107	cgcggagctccgaagtttattattttatgattt
NT108	cgcggatccattaattcaattataccaag
NT109	gtcgagctctattctccattcttttaaaattattatcc
NT110	cacggatcctaagattaccttaatattatacttag
NT111	caggagctcgttgatattaaacttaaaagcaatattattgttg
NT112	gacggatccaacctaacctcaagaattaaataatac
NT113	tatgagctccttgttttcaatgataggttttttagg
NT114	tatggatccatgatgattctaatcataaaaaatcaaaatatc
NT115	tatgagctcggcaatagaagaatctatagaaagc
NT116	cacggatccaatttattataaacttcattgctgttaac
NT160	cgcaagcttatttatataattcatccataccatgagtaatacc
NT161	tatggatccatgagtaaaggtgaagaattatttactggtg
NT169	cagcctaggttaatcttcaataacatgtaaaccacg
NT170	tatcggccgcatggcttgttatgactg
NT171	tatctgcagcatatggctaaacctttaagtcaag
NT172	tatacgcgtaagccgatctcggcttg
NT173	tatcggccgtacccgagcttcaaggaag
NT174	gagcatatgatggaaacctccctcatttaaaattgc
NT187	ctactaaaacattgaacaccccaagttaaagtagtaactaaagtaggccaag
NT188	cttggcctactttagttactactttaacttggggtgttcaatgttttagtag
NT189	tctttacttaatttactttgataacttaaataatgattatcaggtaataaaacaggaccatcac
NT190	gtgatggtcctgttttattacctgataatcattatttaagttatcaaagtaaattaagtaaaga
NT193	cagaagcttatttatataattcatccataccacctg
NT342	tatggatccaggaggttcatggttagtaaaggtgaagaagataatatgg

[a]Restriction enzyme sites are underlined in the primer sequence

III. DNA sequences of genes codon-optimised for translation in *B. burgdorferi*

***bsd*^{Bb}:**

5'ATGGCTAAACCTTTAAGTCAAGAAGAAAGTACTTTAATTGAAAGAGCTACTGCTACTATTAATAGT
ATTCCTATTAGTGAAGATTATAGTGTTGCTAGTGCTGCTTTAAGTAGTGATGGTAGAATTTTTACTGG
TGTTAATGTTTATCATTTTACTGGTGGTCCTTGTGCTGAATTAGTTGTTTTAGGTACTGCCGCCGCTG
CTGCTGCTGGTAATCTCACTTGTATTGTTGCTATTGGTAATGAAAATAGAGGTATTTTAAGTCCTTGT
GGTAGATGTAGACAAGTTTTATTAGATTTACATCCTGGTATTAAAGCTATTGTTAAAGATAGTGATG
GTCAACCTACTGCTGTTGGTATTAGAGAATTATTACCTAGTGGTTATGTTTGGGAAGGTTAA3'

***hph*^{Bb}:**

5'ATGGATAGAAGTGGTAAACCTGAATTAACTGCTACTAGTGTTGAAAAATTTTTAATTGAAAAATTT
GATAGTGTTAGTGATTTAATGCAATTAAGTGAAGGTGAAGAAAGTAGAGCTTTTAGTTTTGATGTTG
GTGGTAGAGGTTATGTTTTAAGAGTTAATAGTTGTGCTGATGGTTTTTATAAAGATAGATATGTTTAT
AGACATTTTGCTAGTGCTGCTTTACCTATTCCTGAAGTTTTAGATATTGGTGAATTTAGTGAAAGTTT
AACTTATTGTATTAGTAGAAGAGCACAAGGTGTTACTTTACAAGATTTACCTGAAACTGAATTACCT
GCTGTTTTACAACCTGTTGCTGAAGCTATGGATGCTATTGCGGCGGCTGATCTCAGTCAAACTTCGG
GTTTTGGTCCTTTTGGTCCTCAAGGTATTGGTCAATATACTACTTGGAGAGATTTTATTTGTGCTATT
GCTGATCCTCATGTTTATCATTGGCAAACTGTTATGGATGATACTGTTAGTGCTAGTGTTGCTCAAGC
ATTAGATGAATTAATGTTATGGGCTGAAGATTGTCCTGAAGTTAGACATTTAGTTCATGCTGATTTTG
GTAGTAATAATGTTTTAACTGATAATGGTAGAATTACTGCTGTTATTGATTGGAGTGAAGCTATGTTT
GGTGATAGTCAATATGAAGTTGCTAATATTTTTTTTTGGAGACCTTGGTTAGCTTGTATGGAACAAC
AAACTAGATATTTTGAAAGAAGACATCCTGAATTAGCTGGTAGTCCTAGATTAAGAGCTTATATGTT
AAGAATTGGTTTAGATCAATTATATCAAAGTTTAGTTGATGGTAATTTTGATGATGCTGCTTGGGCTC
AAGGTAGATGTGATGCTATTGTTAGAAGTGGTGCTGGTACTGTTGGTAGAACTCAAATTGCTAGAAG
AAGTGCTGCTGTTTGGACTGATGGTTGTGTTGAAGTTTTAGCTGATAGTGGTAATAGAAGACCTAGT
ACTAGACCTAGAGCTAAAGAATAA3'

***mCerulean*^{Bb}:**

5'ATGGTTAGTAAAGGTGAAGAATTATTTACTGGTGTTGTTCCTATTTTAGTTGAATTAGATGGTGATG
TTAATGGTCATAAATTTAGTGTTAGTGGTGAAGGTGAAGGTGATGCTACTTATGGTAAATTAACTTT
AAAATTTATTTGTACTACTGGTAAATTACCTGTTCCTTGGCCTACTTTAGTTACTACTTTAACTTGGG
GTGTTCAATGTTTTGCTAGATATCCTGATCATATGAAACAACATGATTTTTTTAAAAGTGCTATGCCT
GAAGGTTATGTTCAAGAAAGGACTATTTTCTTCAAAGATGATGGTAATTATAAAACTAGAGCTGAA
GTTAAATTTGAAGGTGATACTTTAGTTAATAGAATTGAATTAAAAGGTATTGATTTTAAAGAAGATG
GTAATATTTTAGGTCATAAATTAGAATATAATGCTATTAGTGATAATGTTTATATTACAGCTGATAA
ACAAAAAAAATGGTATTAAAGCTAATTTTAAAATTAGACATAATATTGAAGATGGTAGTGTTCAATTA
GCTGATCATTATCAACAAAATACTCCTATTGGTGATGGTCCTGTTTTATTACCTGATAATCATTATTT
AAGTACTCAAAGTAAATTAAGTAAAGATCCTAATGAAAAAAGAGATCATATGGTTTTATTAGAATTT
GTTACTGCTGCTGGTATTACTTTAGGTATGGATGAATTATATAAATAA3'

***msfCFP^{Bb}*:**

5'ATGAGTAAAGGTGAAGAATTATTTACTGGTGTTGTTCCTATTTTAGTTGAATTAGATGGTGATGTTA
ATGGTCATAAATTTAGTGTTAGAGGTGAAGGTGAAGGTGATGCTACTAATGGTAAATTAACTTTAAA
ATTTATTTGTACTACTGGTAAATTACCTGTTCCTTGGCCTACTTTAGTTACTACTTTAACTTGGGGTGT
TCAATGTTTTAGTAGATATCCTGATCATATGAAAAGACATGATTTTTTTAAAAGTGCTATGCCTGAA
GGTTATGTTCAAGAAAGAACTATTAGTTTTAAAGATGATGGTACTTATAAAACTAGAGCTGAAGTTA
AATTTGAAGGTGATACTTTAGTTAATAGAATTGAATTAAAAGGTATTGATTTTAAAGAAGATGGTAA
TATTTTAGGTCATAAATTAGAATATAATTTTAATAGTCATAATGTTTATATTACTGCTGATAAACAAA
AAAATGGTATTAAAGCTAATTTTAAAATTAGACATAATGTTGAAGATGGTAGTGTTCAATTAGCTGA
TCATTATCAACAAAATACTCCTATTGGTGATGGTCCTGTTTTATTACCTGATAATCATTATTTAAGTA
CTCAAAGTAAATTAAGTAAAGATCCTAATGAAAAAAGAGATCATATGGTTTTATTAGAATTTGTTAC
TGCTGCTGGTATTACTCATGGTATGGATGAATTATATAAATAA3'

***mEGFP^{Bb}*:**

5'ATGGTTAGTAAAGGTGAAGAATTATTTACTGGTGTTGTTCCTATTTTAGTTGAATTAGATGGTGATG
TTAATGGTCATAAATTTAGTGTTAGTGGTGAAGGTGAAGGTGATGCTACTTATGGTAAATTAACTTT
AAAATTTATTTGTACTACTGGTAAATTACCTGTTCCTTGGCCTACTTTAGTTACTACTTTAACTTATG
GTGTTCAATGTTTTAGTAGATATCCTGATCATATGAAACAACATGATTTTTTTAAAAGTGCTATGCCT
GAAGGTTATGTTCAAGAAAGGACTATTTTCTTCAAAGATGATGGTAATTATAAAACTAGAGCTGAA
GTTAAATTTGAAGGTGATACTTTAGTTAATAGAATTGAATTAAAAGGTATTGATTTTAAAGAAGATG
GTAATATTTTAGGTCATAAATTAGAATATAATTATAATAGTCATAATGTTTATATTATGGCTGATAA
ACAAAAAAAATGGTATTAAAGTTAATTTTAAAATTAGACATAATATTGAAGATGGTAGTGTTCAATTA
GCTGATCATTATCAACAAAATACTCCTATTGGTGATGGTCCTGTTTTATTACCTGATAATCATTATTT
AAGTACTCAAAGTAAATTAAGTAAAGATCCTAATGAAAAAAGAGATCATATGGTTTTATTAGAATTT
GTTACTGCTGCTGGTATTACTTTAGGTATGGATGAATTATATAAATAA3'

***msfGFP^{Bb}*:**

5'ATGAGTAAAGGTGAAGAATTATTTACTGGTGTTGTTCCTATTTTAGTTGAATTAGATGGTGATGTTA
ATGGTCATAAATTTAGTGTTAGAGGTGAAGGTGAAGGTGATGCTACTAATGGTAAATTAACTTTAAA
ATTTATTTGTACTACTGGTAAATTACCTGTTCCTTGGCCTACTTTAGTTACTACTTTAACTTATGGTGT
TCAATGTTTTAGTAGATATCCTGATCATATGAAAAGACATGATTTTTTTAAAAGTGCTATGCCTGAA
GGTTATGTTCAAGAAAGAACTATTAGTTTTAAAGATGATGGTACTTATAAAACTAGAGCTGAAGTTA
AATTTGAAGGTGATACTTTAGTTAATAGAATTGAATTAAAAGGTATTGATTTTAAAGAAGATGGTAA
TATTTTAGGTCATAAATTAGAATATAATTTTAATAGTCATAATGTTTATATTACTGCTGATAAACAAA
AAAATGGTATTAAAGCTAATTTTAAAATTAGACATAATGTTGAAGATGGTAGTGTTCAATTAGCTGA
TCATTATCAACAAAATACTCCTATTGGTGATGGTCCTGTTTTATTACCTGATAATCATTATTTAAGTA
CTCAAAGTAAATTAAGTAAAGATCCTAATGAAAAAAGAGATCATATGGTTTTATTAGAATTTGTTAC
TGCTGCTGGTATTACTCATGGTATGGATGAATTATATAAATAA3'

***mCitrine*^{Bb}:**

5'ATGGTTAGTAAAGGTGAAGAATTATTTACTGGTGTTGTTCCTATTTTAGTTGAATTAGATGGTGATG
TTAATGGTCATAAATTTAGTGTTAGTGGTGAAGGTGAAGGTGATGCTACTTATGGTAAATTAACTTT
AAAATTTATTTGTACTACTGGTAAATTACCTGTTCCTTGGCCTACTTTAGTTACTACTTTTGGATATG
GTTTAATGTGTTTTGCTAGATATCCTGATCATATGAAACAACATGATTTTTTTAAAAGTGCTATGCCT
GAAGGTTATGTTCAAGAAAGGACTATTTTCTTCAAAGATGATGGTAATTATAAAACTAGAGCTGAA
GTTAAATTTGAAGGTGATACTTTAGTTAATAGAATTGAATTAAAAGGTATTGATTTTAAAGAAGATG
GTAATATTTTAGGTCATAAATTAGAATATAATTATAATAGTCATAATGTTTATATTATGGCTGATAA
ACAAAAAAAATGGTATTAAAGTTAATTTTAAAATTAGACATAATATTGAAGATGGTAGTGTTCAATTA
GCTGATCATTATCAACAAAATACTCCTATTGGTGATGGTCCTGTTTTATTACCTGATAATCATTATTT
AAGTTATCAAAGTAAATTAAGTAAAGATCCTAATGAAAAAAGAGATCATATGGTTTTATTAGAATTT
GTTACTGCTGCTGGTATTACTTTAGGTATGGATGAATTATATAAATAA3'

***msfYFP*^{Bb}:**

5'ATGAGTAAAGGTGAAGAATTATTTACTGGTGTTGTTCCTATTTTAGTTGAATTAGATGGTGATGTTA
ATGGTCATAAATTTAGTGTTAGAGGTGAAGGTGAAGGTGATGCTACTAATGGTAAATTAACTTTAAA
ATTTATTTGTACTACTGGTAAATTACCTGTTCCTTGGCCTACTTTAGTTACTACTTTAACTTATGGTGT
TCAATGTTTTAGTAGATATCCTGATCATATGAAAAGACATGATTTTTTTAAAAGTGCTATGCCTGAA
GGTTATGTTCAAGAAAGAACTATTAGTTTTAAAGATGATGGTACTTATAAAACTAGAGCTGAAGTTA
AATTTGAAGGTGATACTTTAGTTAATAGAATTGAATTAAAAGGTATTGATTTTAAAGAAGATGGTAA
TATTTTAGGTCATAAATTAGAATATAATTTTAATAGTCATAATGTTTATATTACTGCTGATAAACAAA
AAAATGGTATTAAAGCTAATTTTAAAATTAGACATAATGTTGAAGATGGTAGTGTTCAATTAGCTGA
TCATTATCAACAAAATACTCCTATTGGTGATGGTCCTGTTTTATTACCTGATAATCATTATTTAAGTT
ATCAAAGTAAATTAAGTAAAGATCCTAATGAAAAAAGAGATCATATGGTTTTATTAGAATTTGTTAC
TGCTGCTGGTATTACTCATGGTATGGATGAATTATATAAATAA3'

***mCherry*^{Bb}:**

5'ATGGTTAGTAAAGGTGAAGAAGATAATATGGCTATTATTAAAGAATTTATGAGATTTAAAGTTCAC
ATGGAAGGTAGTGTTAATGGTCATGAATTTGAAATTGAAGGTGAAGGTGAAGGTAGACCTTATGAA
GGTACTCAAACTGCTAAATTAAAAGTTACTAAAGGTGGTCCTTTACCTTTTGCTTGGGATATTTTAAG
TCCTCAATTTATGTATGGTAGTAAAGCATACGTTAAACATCCTGCTGATATTCCTGATTATTTAAAAT
TAAGTTTTCCTGAAGGTTTTAAATGGGAAAGAGTTATGAATTTTGAAGATGGTGGTGTTGTTACTGT
TACTCAAGATAGTAGTTTACAAGATGGTGAATTTATTTATAAAGTTAAATTAAGAGGTACTAATTTT
CCTAGTGATGGTCCTGTTATGCAAAAAAAAACTATGGGTTGGGAAGCTAGTAGTGAAAGAATGTAT
CCTGAAGATGGTGCTTTAAAAGGTGAAATTAAACAAAGATTAAAATTAAAAGATGGTGGTCATTAT
GATGCTGAAGTTAAAACTACTTATAAAGCTAAAAAACCTGTTCAATTACCTGGTGCTTATAATGTTA
ATATTAAATTAGATATTACTTCGCATAATGAAGATTATACTATTGTTGAACAATATGAAAGAGCTGA
AGGTAGACATAGTACAGGTGGTATGGATGAATTATATAAATAA3'

***iRFP^{Bb}*:**

5'ATGGCTGAAGGTAGTGTTGCTAGGCAGCCTGACTTATTAACTTGTGACGATGAACCTATTCATATT
CCTGGTGCTATTCAACCTCATGGTTTATTATTAGCTTTAGCTGCTGATATGACTATTGTTGCTGGTAG
TGATAATTTACCTGAATTAACTGGTTTAGCTATTGGTGCTTTAATTGGTAGAAGTGCTGCTGATGTTT
TTGATAGTGAAACTCATAATAGATTAACTATTGCTTTAGCTGAACCTGGTGCTGCTGTTGGTGCTCCT
ATTACTGTTGGTTTTACTATGAGAAAAGATGCTGGTTTTATTGGTAGTTGGCATAGACATGATCAATT
AATTTTTTTAGAATTAGAACCTCCTCAAAGAGATGTTGCTGAACCTCAAGCATTTTTTAGAAGAACT
AATAGTGCTATTAGAAGATTACAAGCTGCTGAAACTTTAGAAAGTGCTTGTGCTGCTGCTGCTCAAG
AAGTTAGAAAAATTACTGGTTTTGATAGAGTTATGATTTATAGATTTGCTAGTGATTTTAGTGGTGA
AGTTATTGCTGAAGATAGATGTGCTGAAGTTGAAAGTAAATTAGGTTTACATTATCCTGCTAGTACT
GTTCCTGCTCAAGCTAGAAGATTATATACTATTAATCCTGTTAGAATTATTCCTGATATTAATTATAG
ACCTGTTCCTGTTACTCCTGATTTAAATCCTGTTACTGGTAGACCTATTGATTTAAGTTTTGCTATTTT
AAGAAGTGTTAGTCCTGTTCATTTAGAATTTATGAGAAATATTGGTATGCATGGTACTATGAGTATT
AGTATTTTAAGAGGTGAAAGATTATGGGGTTTAATTGTTTGTCATCATAGAACTCCTTATTATGTTGA
TTTAGATGGTAGACAAGCATGTGAATTAGTTGCTCAAGTTTTAGCTTGGCAAATTGGTGTTATGGAA
GAATAA3'

IV. Supplementary Table: Numbers of cells analysed to generate quantitative data

Figure	Data point	Number of cells imaged	Strain imaged
Figure 1C	0 μM	121	CJW_Bb100
	0.06 μM	200	
	0.12 μM	207	
	0.25 μM	161	
	0.5 μM	156	
	1 μM	147	
	2 μM	162	
	4 μM	86	
	8 μM	168	
	16 μM	137	
Figure 1D	0 h	78	CJW_Bb100
	1 h	92	
	2 h	110	
	4 h	86	
	6 h	82	
	8 h	103	
	10 h	68	
Figure 2	EV	307	CJW_Bb073
	mCerulean	219	CJW_Bb095
	msfCFP	117	CJW_Bb091
	mEGFP	135	CJW_Bb094
	msfGFP	144	CJW_Bb090
	mCitrine	308	CJW_Bb096
	msfYFP	214	CJW_Bb092
	mCherry	119	CJW_Bb093
	iRFP	209	CJW_Bb100
Figure 3C	EV	134	CJW_Bb069
	P_{0526}	102	CJW_Bb111
	P_{0826}	160	CJW_Bb112
	P_{resT}	148	CJW_Bb108
	P_{0031}	127	CJW_Bb110
	P_{0026}	97	CJW_Bb109
	P_{flaB}	136	CJW_Bb146

V. MATLAB code

The functions CL_getframe.m, CL_removeCell.m, CL_cellId2PositionInFrame.m, and getextradata.m were previously described (6). They are available as part of the open-source, free software package Oufti, which may be downloaded from http://oufti.org/ .

AddMeshtoCellList.m

This script curates the cell list generated by Oufti. It removes cells that do not have meshes, adds extra fields to the cell structures (e.g. area or cell length), and converts area from pixel^2 to μm^2.

```
%********************************************************************************
%%%    removing cells that do not have meshes  %%%%%%
for ii = 1:length(cellList.meshData)
[~,cellIds] = CL_getFrame(ii,cellList);
if cellIds == 0, continue;end
for jj = cellIds
if
~isfield(cellList.meshData{ii}{CL_cellId2PositionInFrame(jj,ii,cellList)},'mesh')
cellList =  CL_removeCell(jj,ii,cellList);
end
end
end
%********************************************************************************

%********************************************************************************
%%%  adding extra fields to cell structures such as area, length, etc %%%%%
for ii = 1:length(cellList.meshData)
for jj = 1:length(cellList.meshData{ii})
cellList.meshData{ii}{jj} = getextradata(cellList.meshData{ii}{jj});
end
end
%**********

cellList = Area_to_microns2(cellList);
```

Area_to_microns2.m

This function converts cell area from pixel^2 to μm^2 using the measured conversion factor 0.0642 μm/pixel that is specific to our microscope setup

```
function cellList = Area_to_microns2(cellList)
%{
-About-
converts the area field of a cellist from pixels^2 to microns^2 given the
conversion unit 0.0642

-Inputs-
cellList: an Oufti cellList with area added

-varargin-
N/A

-Outputs-
cellList: the input cellList with the area field converted to um^2

-Example-
converted_cellList = Area_to_micron2(cellList)

-Supplementary-
N/A

-Keywords-
cellList area

-Dependencies-
N/A

-References-

-Author-
Brad Parry, 2018 June 25
%}

%the number of microns in one pixel
pixel_2_um = 0.0642;

no_conversion_performed = true;
for F = 1:length(cellList.meshData)
    for C = 1:length(cellList.meshData{F})
        if isempty(cellList.meshData{F}{C}) ||
~isfield(cellList.meshData{F}{C},'area') || isempty(cellList.meshData{F}{C}.area)
            continue
        end
        cellList.meshData{F}{C}.area = cellList.meshData{F}{C}.area *
(pixel_2_um^2);
        no_conversion_performed = false;
    end
end
if no_conversion_performed
```

```
315         disp('no area conversion was performed. check that the cellList has the field
316     area')
317     end
318     end
```

CalculateFluorPerCell.m

The function CalculateFluorPerCell uses an Oufti-generated cellList as input (containing the fluorescence signal intensity information that was added in Oufti) and calculates the value of the total cell fluorescence (in arbitrary units) divided by the area of the cell (in μm^2).

```
%This is a short script to determine the distribution of fluorescence per
%unit area on a per cell basis

%Application: Calculating the differences in promoter strength for Bb

function normalized_fluorescence = CalculateFluorPerCell(cellList)
%Determine the average fluorescence per cell
normalized_fluorescence = [];
for ii = 1:length(cellList.meshData)
    for jj = 1:length(cellList.meshData{ii})
        cellList.meshData{ii}{jj} = getextradata(cellList.meshData{ii}{jj});
        if isfield(cellList.meshData{ii}{jj},'area')
            fluor_per_unit_area = sum(cellList.meshData{ii}{jj}.signal1) /
cellList.meshData{ii}{jj}.area;
            normalized_fluorescence{end+1} = fluor_per_unit_area;
        end
    end
end
normalized_fluorescence = cell2mat(normalized_fluorescence);
```

VI. Supplementary references

1. Stewart, P.E., Thalken, R., Bono, J.L. and Rosa, P. (2001) Isolation of a circular plasmid region sufficient for autonomous replication and transformation of infectious Borrelia burgdorferi. *Molecular microbiology*, **39**, 714-721.
2. Elias, A.F., Bono, J.L., Kupko, J.J., 3rd, Stewart, P.E., Krum, J.G. and Rosa, P.A. (2003) New antibiotic resistance cassettes suitable for genetic studies in Borrelia burgdorferi. *Journal of molecular microbiology and biotechnology*, **6**, 29-40.
3. Frank, K.L., Bundle, S.F., Kresge, M.E., Eggers, C.H. and Samuels, D.S. (2003) aadA confers streptomycin resistance in Borrelia burgdorferi. *Journal of bacteriology*, **185**, 6723-6727.
4. Babb, K., McAlister, J.D., Miller, J.C. and Stevenson, B. (2004) Molecular characterization of Borrelia burgdorferi erp promoter/operator elements. *Journal of bacteriology*, **186**, 2745-2756.
5. Bono, J.L., Elias, A.F., Kupko, J.J., 3rd, Stevenson, B., Tilly, K. and Rosa, P. (2000) Efficient targeted mutagenesis in Borrelia burgdorferi. *Journal of bacteriology*, **182**, 2445-2452.
6. Paintdakhi, A., Parry, B., Campos, M., Irnov, I., Elf, J., Surovtsev, I. and Jacobs-Wagner, C. (2016) Oufti: an integrated software package for high-accuracy, high-throughput quantitative microscopy analysis. *Molecular microbiology*, **99**, 767-777.